

Journal of Visualized Experiments

Biaxial Basal Tone and Passive Testing of the Murine Reproductive System Using a Pressure Myograph --Manuscript Draft--

Article Type:	Methods Article - JoVE Produced Video
Manuscript Number:	JoVE60125R1
Full Title:	Biaxial Basal Tone and Passive Testing of the Murine Reproductive System Using a Pressure Myograph
Keywords:	Cervix; Vagina; Extension-Inflation testing; mechanical properties; Women's Health; pelvic floor disorders
Corresponding Author:	Kristin Miller, Ph.D Tulane University New Orleans, Louisiana UNITED STATES
Corresponding Author's Institution:	Tulane University
Corresponding Author E-Mail:	kmille11@tulane.edu
Order of Authors:	Shelby E. White Cassandra K. Conway Gabrielle L. Clark Dylan J. Lawrence Carolyn L. Bayer Kristin S. Miller, Ph.D
Additional Information:	
Question	Response
Please indicate whether this article will be Standard Access or Open Access.	Standard Access (US\$2,400)
Please indicate the city, state/province, and country where this article will be filmed . Please do not use abbreviations.	New Orleans, Louisiana



Kristin S. Miller, Ph.D.
Assistant Professor
Department of Biomedical Engineering

Office: 504-988-9324
Cell: 713-503-4878
Kmille11@tulane.edu

Dr. Nandita Singh
Senior Science Editor, *Journal of Visualized Experiments*
1 Alewife Center #200
Cambridge, MA 02140

April 12, 2019,

Dr. Singh,

We are submitting the manuscript titled “Biaxial Basal Tone and Passive Testing of the Murine Reproductive System Using a Pressure Myograph” for consideration of publication as an original article and video production in the *Journal of Visualized Experiments*. This manuscript contains original research that presents the protocol of biaxially testing the murine vagina and cervix in both the basal and passive state while under physiological conditions.

This research has not been previously considered for publication elsewhere and will remain so until the decision is made. All authors have contributed to the article and agreed to submission to the *Journal of Visualized Experiments*. There are no conflicts of interest to be declared with this work.

Thank you for the consideration of our work.

Sincerely,

Kristin S. Miller, Ph.D.

A handwritten signature in black ink that reads 'Kristin S. Miller'.

Corresponding Author
Kristin S. Miller, Ph.D.
Department of Biomedical Engineering, Tulane University
6823 St. Charles Ave, New Orleans, LA 70118 USA
kmille11@tulane.edu, (504) 988-9324

TITLE:

Biaxial Basal Tone and Passive Testing of the Murine Reproductive System Using a Pressure Myograph

AUTHORS AND AFFILIATIONS:

Shelby E. White¹, Cassandra K. Conway¹, Gabrielle L. Clark¹, Dylan J. Lawrence¹, Carolyn L. Bayer¹
Kristin S. Miller¹

¹Department of Biomedical Engineering, Tulane University, New Orleans, LA, USA

Corresponding Author:

Kristin S. Miller (Kmille11@tulane.edu)

Email Addresses of Co-authors:

Shelby White (Swhite18@tulane.edu)

Cassandra K. Conway (cconway2@tulane.edu)

Gabrielle L. Clark (gclark2@tulane.edu)

Dylan J. Lawrence (dlawren@tulane.edu)

Carolyn L. Bayer (Carolynb@tulane.edu)

KEYWORDS:

cervix, vagina, extension-inflation testing, mechanical properties, women's health, pelvic floor disorders

SUMMARY:

This protocol utilized a commercially available pressure myograph system to perform pressure myograph testing on the murine vagina and cervix. Utilizing media with and without calcium, the contributions of the smooth muscle cells (SMC) basal tone and passive extracellular matrix (ECM) were isolated for the organs under estimated physiological conditions.

ABSTRACT:

The female reproductive organs, specifically the vagina and cervix, are composed of various cellular components and a unique extracellular matrix (**ECM**). Smooth muscle cells exhibit a contractile function within the vaginal and cervical walls. Depending on the biochemical environment and the mechanical distension of the organ walls, the smooth muscle cells alter the contractile conditions. The contribution of the smooth muscle cells under baseline physiological conditions is classified as a basal tone. More specifically, a basal tone is the baseline partial constriction of smooth muscle cells in the absence of hormonal and neural stimulation. Furthermore, the ECM provides structural support for the organ walls and functions as a reservoir for biochemical cues. These biochemical cues are vital to various organ functions, such as inciting growth and maintaining homeostasis. The ECM of each organ is composed primarily of collagen fibers (mostly collagen types I, III, and V), elastic fibers, and glycosaminoglycans/proteoglycans. The composition and organization of the ECM dictate the mechanical properties of each organ. A change in ECM composition may lead to the development of reproductive pathologies, such as pelvic organ prolapse or premature cervical remodeling. Furthermore, changes in ECM

microstructure and stiffness may alter smooth muscle cell activity and phenotype, thus resulting in the loss of the contractile force.

In this work, the reported protocols are used to assess the basal tone and passive mechanical properties of the nonpregnant murine vagina and cervix at 4-6 months of age in estrus. The organs were mounted in a commercially available pressure myograph and both pressure-diameter and force-length tests were performed. Sample data and data analysis techniques for the mechanical characterization of the reproductive organs are included. Such information may be useful for constructing mathematical models and rationally designing therapeutic interventions for women's health pathologies.

INTRODUCTION:

The vaginal wall is composed of four layers, the epithelium, lamina propria, muscularis, and adventitia. The epithelium is primarily composed of epithelial cells. The lamina propria has a large amount of elastic and fibrillar collagen fibers. The muscularis is also composed of elastin and collagen fibers but has an increased amount of smooth muscle cells. The adventitia is comprised of elastin, collagen, and fibroblasts, albeit in reduced concentrations compared to the previous layers. The smooth muscle cells are of interest to biomechanically motivated research groups as they play a role in the contractile nature of the organs. As such, quantifying the smooth muscle cell area fraction and organization is key to understanding the mechanical function. Previous investigations suggest that the smooth muscle content within the vaginal wall is primarily organized in the circumferential and longitudinal axis. Histological analysis suggests that the smooth muscle area fraction is approximately 35% for both the proximal and distal sections of the wall¹.

The cervix is a highly collagenous structure, that until recently, was thought to have minimal smooth muscle cell content^{2,3}. Recent studies, however, have suggested that smooth muscle cells may have a greater abundance and role in the cervix^{4,5}. The cervix exhibits a gradient of smooth muscle cells. The internal os contains 50-60% smooth muscle cells where the external os only contains 10%. Mouse studies, however, report the cervix to be composed of 10-15% smooth muscle cells and 85-90% fibrous connective tissue with no mention of regional differences⁶⁻⁸. Given that the mouse model differs from the frequently reported human model, further investigations concerning the mouse cervix are needed.

The purpose of this protocol was to elucidate the mechanical properties of the murine vagina and cervix. This was accomplished by using a pressure myograph device that enables assessment of mechanical properties in the circumferential and axial directions simultaneously while maintaining native cell-matrix interactions and organ geometry. The organs were mounted on two custom cannulas and secured with silk 6-0 sutures. Pressure-diameter tests were performed around the estimated physiological axial stretch to determine the compliance and tangent moduli⁹. Force-length tests were conducted to confirm the estimated axial stretch and to ensure that mechanical properties were quantified in the physiological range. The experimental protocol was performed on the nonpregnant murine vagina and cervix at 4-6 months of age in estrus.

The protocol is divided into two main mechanical testing sections: basal tone and passive testing. A basal tone is defined as the baseline partial constriction of smooth muscle cells, even in the absence of external local, hormonal, and neural stimulation¹⁰. This baseline contractile nature of the vagina and cervix yields characteristic mechanical behaviors which are then measured by the pressure myograph system. The passive properties are assessed by removing the intercellular calcium that maintains the baseline state of contraction, resulting in relaxation of the smooth muscle cells. In the passive state, collagen and elastin fibers provide the dominant contributions for the mechanical characteristics of the organs.

The murine model is used extensively to study pathologies in women's reproductive health. The mouse offers several advantages for quantifying the evolving relationships between ECM and mechanical properties within the reproductive system¹¹⁻¹⁴. These advantages include short and well-characterized estrous cycles, relatively low cost, ease of handling, and a relatively short gestational time¹⁵. Additionally, the genome of laboratory mice is well-mapped and genetically-modified mice are valuable tools to test mechanistic hypotheses¹⁶⁻¹⁸.

Commercially available pressure myograph systems are used extensively to quantify the mechanical responses of various tissues and organs. Some notable structures analyzed on the pressure myograph system include elastic arteries¹⁹⁻²², veins and tissue engineered vascular grafts^{23,24}, the esophagus²⁵, and the large intestines²⁶. The pressure myograph technology permits simultaneous assessment of properties in the axial and circumferential directions while maintaining the native cell-ECM interactions and in vivo geometry. Despite the extensive use of myograph systems in soft tissue and organ mechanics, a protocol utilizing the pressure myograph technology had not previously been developed for the vagina and cervix. Prior investigations into the mechanical properties of the vagina and cervix were assessed uniaxially^{27,28}. These organs, however, experience multiaxial loading within the body^{29,30}, thus quantifying their biaxial mechanical response is important.

Moreover, recent work suggests smooth muscle cells may play a potential role in soft tissue pathologies^{5,28,31,32}. This provides another attraction of utilizing the pressure myograph technology, as it preserves the native cell-matrix interactions, thus permitting delineation of the contribution that smooth muscle cells play in physiological and pathophysiological conditions. Herein, we propose a protocol to quantify the multiaxial mechanical properties of the vagina and cervix under both basal tone and passive conditions.

PROTOCOL:

Nulliparous 4-6 months female C57BL6J mice (29.4 ± 6.8 grams) at estrus were used for this study. All procedures were approved by the Institute Animal Care and Use Committee at Tulane University. After delivery, the mice acclimated for one week before euthanasia and were housed under standard conditions (12-hour light/dark cycles).

1. Mouse sacrifice at estrus

1.1. Determine the estrous cycle: The estrous cycle was monitored by visual assessment in accordance to previous studies^{15,33,34}. The estrous cycle consists of four stages: proestrus, estrus, metestrus, and diestrus. During the proestrus phase the genitals are swollen, pink, moist, and wrinkled. The estrus phase is wrinkly but less swollen, pink, and moist. Metestrus and diestrus are both reported as exhibiting no swelling and wrinkling, lacking in a pink hue, and dry^{34,35}.

1.2. Perform experiment at estrus: All mechanical tests were performed while the mice were at estrus, as this is the easiest to visualize and provides a consistent and repeatable timepoint.

1.3. For mice undergoing basal tone testing, euthanize via guillotine. For mice tested only under the passive conditions, euthanize using carbon dioxide (CO₂) inhalation. The guillotine serves to preserve the function of smooth muscle cells of the reproductive tract, as the CO₂ gas alters the contractile properties of the smooth muscle cells³⁶⁻⁴². It is imperative to perform the dissection within 30 minutes to minimize the chance of cell apoptosis.

2. Reproductive system dissection

2.1. Set up: Place an absorbent pad on the workstation and fill a Petri dish and syringe with 4 °C Hank's Balanced Salt Solution (HBSS) solution. Use a wipe for adipose tissue disposal. Place the mouse ventral side up and tape the paws and tail. Turn the microscope lights on and set out micro-scissors, scissors, two pairs of straight tweezers, and two pairs of curved tweezers.

2.2. Using angled tweezers and scissors, lift the skin around the abdomen and make an incision at the base of the abdomen, above the pubic bone. The incision should be shallow enough to not puncture the abdominal muscle wall. Continue using the scissors to cut superiorly towards the rib cage and deep through the abdominal muscles.

2.3. Remove superficial fat by pulling lightly on the fat with the curved tweezers and micro-scissors. Adipose tissue will reflect light heterogeneously with a glitter-like appearance. Place all the removed fat and tissue on the wipe. Identify both uterine horns and the pubic bone.

2.4. Place closed scissors between the vaginal wall and the pubic bone. Carefully cut the middle of the pubic bone (pubic symphysis). Place curved tweezers on both ends of the cut pubic bone. Pull both cut ends laterally to allow for better access to the reproductive organs.

2.5. Remove the bladder and the urethra from the vaginal wall. This can be done by using straight tweezers and micro-scissors. Hold the bladder with straight tweezers to create tension and use blunt dissection techniques to separate the surrounding tissue from the vagina. Once the bladder and urethra are dissected away, cut the base and remove from the body cavity.

2.6. Identify the reproductive system: The uterine horns bifurcate from the cervix. The cervix can be identified from the vagina due to differences in geometry and stiffness. The outer diameter of the cervix is smaller than the vagina. The cervix is stiffer than the vagina and feels similar to that of a bead (**Figure 1**).

2.7. Use ink and calipers to mark 3 mm dots along the organs. Start below the ovaries on the uterine tubes and mark dots inferiorly to reach the cervix. Use the center cervix dot to start a dot path down to the vagina introitus.

2.8. Allow the ink to dry and separate the reproductive organs from surrounding adipose tissue, connective tissue, and the colon. Clean the vagina as close to the vaginal introitus as possible. Using scissors, cut around the vaginal introitus.

NOTE: It is possible for organs to dry out during this process. If this is a concern, a syringe filled with 4 °C HBSS may be used to add moisture to the organs.

2.9. Cut the uterine horns immediately inferior to the ovaries. Note that the organs will retract from the post explant length as the connective tissue is removed and the organ recoils. Place the dissected reproductive organs in a Petri dish filled with 4 °C HBSS. This change in length can be used in for calculating the estimated in vivo length (section 5).

NOTE: We have identified that using HBSS at this temperature during the dissection and cannulation does not affect the smooth muscle cell viability. Maintaining a pH of 7.4, however, is imperative for maintaining the viability of the smooth muscle cells. At this temperature, the HBSS has a pH level of 7.4.

2.10. After a 15-minute equilibration period in 4 °C HBSS, measure the space between dots using calipers. Record the measurements for each distance into a spreadsheet. These values will be used to calculate the in vivo stretch ratio (original length/explanted length).

2.11. Set the wipe that contains the discarded tissue on the abdominal region with the excess tissue facing the inside of the mouse and soak the wipe in 4 °C HBSS. Wrap the mouse and excess tissue in foil and place in a freezer safe bag to be stored at -20 °C. Passive mechanical behavior on the vagina was not found to be significantly different after one freeze-thaw cycle⁴³. All organs tested were used immediately after euthanasia or after one freeze-thaw cycle.

3. Cannulating

3.1. Determine the proper cannula size for the organ type. In a typical C57BL6J mouse, the vagina uses cannulas that are both 3.75 mm in diameter and riveted. The cervix uses one cannula that is 3.75 mm for the vaginal end and a cannula 0.75 mm in diameter for the uterine end (**Figure 2**) The 0.75 mm cannula is smooth.

NOTE: The diameter sizes denoted above are used for typical nulliparous 4-6 months C57-BL/6 mice, C57BL/6 x 129SvEv, and nonparous mice aged 4-6 months. However, certain circumstances, such as prolapse or pregnancy, may require a larger size cannula.

3.2. With each organ, mount the cervical side on the force transducer portion of the cannulation device. Mount the opposite end of the organ (vaginal or uterine) on the micrometer portion of the device. Tighten both ends with sutures.

3.3. Due to the difference in thickness and degree of contractility among the vagina and cervix, varying techniques may be utilized to perform the most effective cannulation. For the vagina, place 3 sutures in between the 2nd and 3rd rivets of the cannula in a “X” fashion. When cannulating the cervix, the cannula is not riveted so the organ is best placed at the back of the cannula with 3 horizontal sutures on the uterine end and 4 sutures on the external os. For both organs, maximum length should be no more than 7 mm between the sutures (**Figure 3**).

4. Pressure myograph set up

4.1. In order to set up the pressure myograph system, power on the testing system and fill the reservoir bottle with 200 mL of HBSS (**Figure 4**). Turn the heat to “on” and allow the HBSS in the reservoir bottle to heat up. Next, turn on the microscope and open the computer program. Ensure that the image of the cannulated organ, pressure interface, flow meter readings, and the sequencer function tool are all visible (**Figure 5**).

5. Basal tone mechanical testing

NOTE: The cervix exhibited a phasic nature during the beginning stages of testing. However, this diminished after preconditioning. Basal tone testing is done utilizing Krebs Ringer Buffer (KRB) in the basin of the DMT device. The buffer is aerated with 95% O₂ and 5% CO₂. After the basal tone portion is complete, calcium free KRB is utilized.

5.1. Finding the unloaded geometry: Stretch the organ so that the wall is not in tension. For the vagina, observe the grooves on the vaginal wall. For the cervix, cut immediately below the ink dots that located above and below the central cervix mark. This devises a repeatable method for a cervical in situ length of 6 mm⁴⁴. Measure the length from suture to suture with calipers

5.2. Finding the unloaded pressure (UP): Increase the pressure from 0 to 10 mmHg in increments of 1 mmHg. Determine the pressure in which the organ is no longer collapsed. This can be determined as the largest jump in the outer diameter at a given pressure, as exhibited on the program monitor. After recording the pressure and outer diameter, note this as the first point wherein the organ is not collapsed and zero the force.

5.3. Estimated in vivo stretch: Calculate the estimated in vivo stretch by dividing the length measured in vivo by the length measured post explant:

$$\lambda_{iv} = l_{in\ vivo} / l_{post-explant}$$

5.4. Pressure-diameter pre-conditioning: Set the pressure to 0 mmHg, the length to the estimated in vivo length and the gradient to 1.5 mmHg/s. Run a sequence that takes the pressure from 0 mmHg to the in vivo pressure + unloaded (**Table 1**), hold for 30 seconds, and take the pressure to 0 mmHg with a 30 second hold period. After repeating for a total of 5 cycles, press **Stop** in the computer program and save the file.

5.5. Finding the experimental in vivo stretch: Adjust the organ to be at the estimated in vivo length while at the unloaded pressure and press **Start**. Assess pressure vs force values for pressure values ranging from the unloaded pressure to the maximum pressure (**Table 1**). Press the **Stop** button in the computer program and save the file.

NOTE: The measured stretch value is calculated in situ. This is accompanied by the limitation that it can only be measured after disarticulating the pubic symphysis. As a result, the natural tethering is lost, which may modify the length. The theoretical stretch, however, is based on the previously introduced theory that the organ will experience minimal changes in force when exposed to physiological pressures to conserve energy⁴⁵. In the protocol, the measured in vivo stretch will be the stretch value calculated using the experimentally identified length wherein there is minimal change in force when exposed to a physiological range of pressures.

5.6. Pressure-diameter pre-conditioning: Set the pressure to 0 mmHg, the length to the experimental in vivo length, and the gradient of 1.5 mmHg/s. Run a sequence that takes the pressure from 0 mmHg to the maximum pressure + UP, hold for 30 seconds, and back to 0 mmHg with an additional 30 second hold period. After repeating this for a total of 5 cycles, press the **Stop** button in the program interface and save the file.

NOTE: 5.4 is imperative for achieving a more consistent axial force reading with increasing pressure. This step aids in finding the correct in vivo stretch, which is often underestimated based on visual cues. 5.6 serves as a precautionary step to minimize hysteresis and to achieve a consistent, repeatable, mathematically interpretable response of the organ.

5.7. Force-length pre-conditioning: Enter 1/3 max pressure + UP for both the inlet and outlet pressure. Adjust the organ to -2% of the in vivo length and press **Start**. Adjust the length to +2% in vivo length then back down to -2% at 10 μ m/s. Repeat axial extension for a total of 5 cycles. Press **Stop** in the computer program and save the file.

5.8. Equilibration: With the organ at the determined in vivo length, set both the inlet and outlet pressure at 1/3 of the maximum pressure + UP. Equilibrate the organ for 10 minutes. Slowly bring both pressures back down to 0 mmHg with the gradient set as 1.5 mmHg/s.

5.9. Re-evaluate the unloaded geometry: Set the organ to the in vivo length and the pressure to the unloaded pressure. Decrease the axial length towards the estimated unloaded length at a rate of 10 μ m/s until there is minimal change in the force. This corresponding length is known as the unloaded length, or where the organ is not in tension nor compression. Before zeroing the force, record the unloaded length, outer diameter, and the force value.

NOTE: The prior unloaded geometry was determined by visual cues, which is purely qualitative. A re-evaluation is necessary for a quantitative method and to account for possible changes in length that may occur during the preconditioning. This geometry will be used in section 8.

5.10. Ultrasound Setup: Use the general imaging abdominal package to visualize the organs in the testing device. (**Figure 6**). Before testing, minimize artifacts from the bottom of the pressure myograph metal basin. Adjust the cannula to a height that is the maximum distance from the bottom with the tissue still being fully submerged in the testing solution. A custom holder is 3D printed to stabilize the transducer in a vertical position during imaging.

5.11. Ultrasound Imaging: Identify the cannula near the force transducer and adjust the stage of the microscope to image along the length of the tissue. Throughout the testing process, the middle region along the length is tracked (**Figure 6A,C**). Following imaging, review the image “Cine store” loop that consists of a series of B-mode frames and identify the frame with the largest outer diameter. The thickness calculations made will be used in section 8.

5.12. Pressure diameter testing (-2% in vivo length): Press **Start** and adjust the organ so that it is -2% of the in vivo length, set the pressure to 0 mmHg and gradient to 1.5 mmHg/s. Increase the pressure from 0 mmHg to the maximum pressure. Bring the pressure back down to 0 mmHg with a 20 second hold period. Repeat this for 5 cycles.

5.13. Pressure diameter testing (in vivo length): Press **Start** and adjust the organ so that it is at the vivo length, set the pressure to 0 mmHg, and gradient to 1.5 mmHg/s. Increase the pressure from 0 mmHg to the maximum pressure. Bring the pressure back down to 0 mmHg with a 20 second hold period. Repeat this for 5 cycles.

5.14. Pressure diameter testing (+2% in vivo length): Adjust the organ so that it is +2% in vivo length, set the pressure to 0 mmHg, and gradient to 1.5 mmHg/s. Increase the pressure from 0 mmHg to the maximum pressure and then back down to 0 mmHg with a 20 second hold period. Repeat this for 5 cycles. The pressure data from all three lengths will be used in section 8.

5.15. Force-length testing (Nominal pressure): Set the pressure to the unloaded pressure and the organ to -2% of the in vivo length. Stretch the organ to +2% of the in vivo length and return to -2% the in vivo length at rate of 10 $\mu\text{m/s}$. Repeat for a total of 3 cycles.

5.16. Force-length testing (1/3 maximum pressure + UP): Set the pressure to 1/3 of the maximum pressure + UP and adjust the organ to -2% the in vivo length. After pressing **Start**, stretch the organ to +2% the in vivo length and back to -2% the in vivo length at a rate of 10 $\mu\text{m/s}$. After repeating for a total of 3 cycles, press **Stop** and save the data.

5.17. Force-length testing (2/3 maximum pressure + UP): Set the pressure to 2/3 of the maximum pressure + UP and adjust the organ to -2% the in vivo length. Press **Start** and stretch the organ to

+2% the in vivo length and back to -2 the in vivo length at a rate of 10 $\mu\text{m/s}$. After repeating for a total of 3 cycles, press **Stop** and save the data.

5.18. Force-length testing (maximum pressure + UP): Set the pressure to the maximum pressure + UP and adjust the organ to -2% the in vivo length. At a rate of 10 $\mu\text{m/s}$, stretch the organ to +2% of the in vivo length and back to -2% the in vivo length. After repeating for a total of 3 cycles, save the data. All force data will be used in section 8.

5.19. Remove KRB testing media and wash with calcium-free KRB. Replace the media with calcium free KRB solution supplemented with 2 mM EGTA. Incubate the tissue for 30 minutes. Remove the solution and replace the media with fresh calcium-free KRB.

6. Passive mechanical testing

NOTE: If starting with passive testing start at step 1. If basal tone testing was performed prior to passive start at step 6. If starting with frozen tissue, allow a 30-minute equilibration period at room temperature before cannulating the organ.

6.1. Finding the unloaded geometry: Stretch the organ so the wall of the organ is not in tension. Measure the cannulated organ from suture to suture and record this as the unloaded length.

6.2. Finding the unloaded pressure: After pressing **Start**, increase the pressure from 0 to 10 mmHg in increments of 1 mmHg. While going through this process, determine the pressure in which the organ is not in tension. Using the computer program monitor, this can be determined from the largest jump in the outer diameter. After zeroing the force, record this pressure as well as the outer diameter and note this as the first point in which the organ is not collapsed.

6.3. Estimated in vivo stretch: Calculate the estimated in vivo stretch by dividing the length measured in vivo by the length measured post-explant.

6.4. Pressure diameter pre-conditioning: After pressing **Start**, set the pressure set to 0 mmHg, the length as the estimated in vivo length, and gradient to 1.5 mmHg/s. Begin running a sequence that takes the pressure from 0 mmHg to the maximum pressure and back to 0 mmHg. Repeat this process through 5 cycles with a 30 second hold time.

6.5. Force-length preconditioning: Adjust the organ to the in vivo length and manually enter the unloaded pressure in the computer program for both pressures. After pressing **Start**, set the gradient to 2 mmHg and the pressure to 1/3 of the maximum. Stretch the organ up to +4% and back down to -4% stretch at 10 $\mu\text{m/s}$. Repeat this cycle for a total of 5 times and press **Stop**.

6.6. Finding the experimental in vivo length: Find and plot force values at -4% of the in vivo length, the in vivo length, and +4% of the in vivo length. Take forces at evenly spaced pressures ranging from 0 mmHg to the maximum pressure. The experimental in vivo stretch will be the stretch value that exhibits a relatively flat line over a range of pressures.

393
394 6.7. Repeat the pressure diameter and axial pre-conditioning steps at the new in vivo length.
395

396 6.8. Equilibration: With the organ at the determined in vivo length, set the inlet and outlet
397 pressure to the unloaded pressure. Let the organ re-equilibrate for 15 minutes. After 15 minutes,
398 slowly bring the inlet and outlet pressure back down to 0 mmHg.
399

400 6.9. Re-evaluate unloaded configuration: Bring the organ to the unloaded length and re-estimate
401 the unloaded length. Record the unloaded length and the outer diameter while the pressure is 0
402 mmHg, the unloaded pressure, and 1/3 the maximum pressure. Zero the force at the unloaded
403 pressure. The diameter at the unloaded pressure is the in vivo diameter.
404

405 NOTE: Re-estimating the unloaded length is necessary as small plastic deformations were
406 observed previously in soft biological tissues following preconditioning. This unloaded
407 configuration will be the one utilized in section 8.
408

409 6.10. Ultrasound: Perform ultrasound B-mode imaging at the unloaded length and pressure.
410

411 6.11. Pressure-diameter testing: With the organ at -2% of the experimentally determined in vivo
412 length and the pressure at 0 mmHg, press **Start**. Increase the pressure from 0 mmHg to the
413 maximum pressure and back to 0 mmHg. Hold the 2-0 mmHg step for 20 seconds. After repeating
414 for a total of 5 times, press the **Stop** button in the interface and save the file.
415

416 NOTE: Repeat at the experimental in vivo length, +2% of the experimental in vivo length.
417

418 6.12. Force-length testing: Set the pressure to nominal pressure and adjust the organ to -2% of
419 the in vivo length. Stretch the organ up to +2% of the in vivo length and back to -2% of the in vivo
420 length at a rate of 10 $\mu\text{m/s}$. After repeating for a total of 3 times, save the data. Repeat this for
421 1/3 max pressure, 2/3 max pressure, and at the max pressure.
422

423 6.13. Calculate the unloaded thickness from ultrasound images B-mode image. Using imaging
424 software, draw a line to denote the penetration depth. Set the scale to the length of the line (i.e.,
425 2000 μm as shown in **Figure 6B and 6D**).
426

427 6.14. Wall thickness calculations: Using a computer software, trace and measure the inner and
428 outer diameter of the organ. Then, draw and measure a line between the diameters. Draw a total
429 of 25 transmural lines. Average all data points and repeat for a total of 3 times.
430

431 7. Clean up 432

433 7.1. Ensure that the pressure is 0 mmHg and turned off. Close the main inlet and outlet off for
434 both three-way valves. Aspirate the remaining fluid from the basin of the cannulation device.
435

7.2. Remove the organ from the stage and fill the reservoir bottle with deionized water. Using a syringe, rinse the cannula with water. Connect the tubing to bypass the cannula.

7.3. Turn the pressure and flow on, set the inlet pressure to 200 mmHg, the outlet pressure to 0 mmHg, gradient to 10 mmHg/s, and let the flow run for 5 minutes. Allow the system to run while the reservoir bottle is empty and let the air run for 5 minutes or until the lines are dry.

8. Data analysis

8.1. For pressure diameter testing, collect data from where the pressure begins to decrease from the maximum value until the end point. For force-length testing, collect data from just below the maximum peak in force until the force stopped decreasing.

8.2. Open the data file for each pressure-diameter test and select the mean pressure tab. Navigate to the loading region of the last curve, 0 mmHg to the maximum pressure, and drop the data into a spreadsheet. Select the same region on the outer diameter, inlet pressure, outlet pressure, force, temperature, pH, and flow tab placing each item in the same document.

8.3. Open the data for each Force-length test. Navigate to the loading region of the curve, -2% to +2%, and drag and drop the data into a spreadsheet. Select the same region for the other measured variables and place each item in the same spreadsheet.

8.4. For the pressure diameter and force length test subtract the UP from all pressure values.

8.5. Average the pressure-diameter data every 1 mmHg (i.e., 0+/- 0.5, 1+/-0.5, 2+/- 0.5).

8.6. Find the unloaded volume of the organ (V). Equation 1 can be utilized to find V , given that R_0^2 is the unloaded outer radius measured by the microscope, L is the unloaded length, and H is the unloaded thickness as detected by the ultrasound. The assumption of incompressibility is leveraged, meaning that the organ conserves volume while subjected to deformations.

NOTE: The unloaded length is measured with calipers from suture to suture. The unloaded diameter is measured via the microscope, camera, and software followed by calculation of the radius (**Figure 5**) The unloaded thickness is calculated from the ultrasound images (**Figure 6**).

$$V = \pi(R_0^2 - (R_0 - H)^2)L \quad \text{Equation 1}$$

8.7. Using the assumption of incompressibility, use the unloaded volume, deformed outer radius (r_0), and length (l) to determine the deformed inner radius (r_i).

$$r_i = \sqrt{r_0^2 - \frac{V}{\pi l}} \quad \text{Equation 2}$$

8.8. Use Equations 3, 4, and 5 to calculate each stress, respectively. In equations 3-5, P is defined as the intraluminal pressure and F_t is the force measured by the transducer.

$$\sigma_{\theta} = \frac{Pr_i}{r_0 - r_i} \quad \text{Equation 3}$$

$$\sigma_z = \frac{F_t + \pi Pr_i^2}{\pi(r_0^2 - r_i^2)} \quad \text{Equation 4}$$

$$\sigma_r = \frac{Pr_i}{r_0 + r_i} \quad \text{Equation 5}$$

8.9. Plot the pressure-diameter relationship, force-pressure relationship, circumferential stress-circumferential stretch relationship, and the axial stress and circumferential stretch values (**Figure 7, Figure 8**). The stretch values can be calculated using the midwall radius. Calculations of the circumferential and axial stresses can be found in Equations 6 and 7, respectively.

$$\lambda_{\theta} = \frac{r_i + r_0 / 2}{R_1 + R_0 / 2} \quad \text{Equation 6}$$

$$\lambda_z = \frac{l}{L} \quad \text{Equation 7}$$

8.10. Calculate compliance near the physiological pressure range and at the in vivo stretch. The lower pressure bound (LPB) is 1 standard deviation below the mean measured pressure. The upper pressure bound (UPB) is 1 standard deviation above the mean measured pressure⁹.

$$\frac{r_o^{UPB} - r_o^{LPB}}{p^{UPB} - p^{LPB}}$$

8.11. Calculate the tangent moduli to quantify the material stiffness. Identify the calculated circumferential stress that corresponds to the lower pressure bound and upper bound pressure. Fit a linear line to the circumferential stress- circumferential stretch curve within the identified stress range at the in vivo length. Calculate the slope of the line⁹.

REPRESENTATIVE RESULTS:

Successful analysis of the mechanical properties of the female reproductive organs is contingent on appropriate organ dissection, cannulation, and testing. It is imperative to explant the uterine horns to the vagina without any defects (**Figure 1**). Depending on the organ type, the cannula size will vary (**Figure 2**). Cannulation must be done so that the organ cannot move during the experiment but also not damage the wall of the organ during the procedure (**Figure 3**). Failure of either step will result in inability of the vessel to hold pressure. Testing procedure standardization is vital to the success of the protocol in order to yield consistent and repeatable results.

Once the organ is dissected and cannulated properly, power on the pressure myograph system. The setup of the pressure myograph systems involves a controller unit, flow meter, and stage (**Figure 4**). The pressure myograph system is used to monitor various aspects of the organ as it undergoes mechanical testing (**Figure 5**). An ultrasound system, or equivalent, is used to measure the thickness of the organs in the unloaded state with and without basal tone (**Figure 6**). After

mechanical testing, the tangent moduli may be calculated for the circumferential and axial directions (**Table 2**).

Both basal tone testing and passive testing yield key mechanical properties of the reproductive tract, with and without the contractile contribution of smooth muscle cells (**Figure 7, Figure 8**). Scaling between the organs requires a few adjustments to the protocols (**Table 1**), as the cervix and vagina experience different loads in vivo⁴⁶⁻⁴⁸. Such variations may be monitored through techniques such as pressure catheterization. Pressure catheterization is a method used previously to monitor the in vivo conditions within the vagina and uterus⁴⁹⁻⁵³. Models in the previous studies range from mice, rabbits, and humans. The same principles would apply similarly to the cervical and vaginal pressure specific for the murine model. Though, regardless which organ is being tested, the same materials are needed for the protocols (**Table 3**).

FIGURE AND TABLE LEGENDS:

Figure 1: Murine dissection diagram. The mouse dissection for the reproductive organs: both uterine horns, cervix, and the vagina. In the figure, the bladder and urethra are removed from the anterior of the vagina. The intestines and abdominal muscles were reflected superiorly.

Figure 2: Size comparison of the two cannula. Size comparison of the two cannulas used for cannulation of the reproductive organs. The larger cannula ($D = 3.75$ mm) is used for the vaginal tissue (**A**). The smaller cannula ($D = 0.75$ mm) is used for cannulating cervical tissue (**B**). The cervical cannula is smooth while the vaginal cannula has two grooves.

Figure 3: Cannulation method for vagina and cervix. Due to the varying geometry and thickness of the reproductive organs, they are most effectively cannulated in distinct manners. For the vagina, place two sutures in an "X" fashion with a third directly at the intersection of the "X". When cannulating the cervix, place 3 horizontal sutures on the uterine end and 4 sutures on the external os.

Figure 4: Setup for pressure myograph device. The setup of the DMT device utilized for both basal and passive testing. The DMT is composed of three main hubs: the stage (**A**), controller unit (**B**), and flow meter (**C**). Within the controller unit, there is a reservoir bottle and a waste bottle. The reservoir bottle is initially filled with fluid that empties as the experiment is carried out. The waste bottle, which is initially empty, collects the fluid that runs through the experiment. The controller unit interfaces with the DMT software on the computer and controls the pressure, temperature, and flow. The controller unit reads the outputs from the force and pressure transducers within the stage through a VGA interface cable. The stage component of the system contains an inlet and outlet flow of the system. The inlet and outlet flow have corresponding inlet and outlet pressures measured by the system.

Figure 5: File setup on the pressure myograph program. Display of computer software set-up. A box is drawn around the region of interest and outer diameter of the tissue is optically tracked in real-time (**A**). Data obtained during mechanical testing is recorded and displayed real-time in the outer diameter, inlet pressure, outlet pressure, mean pressure, force, temperature, pH, and flow

tab (B). Within the pressure interface pressure (mmHg), gradient (mmHg/g), and flow is controlled. Further, the axial force (mN) measured by the in-line force transducer is displayed. Flow rate ($\mu\text{L}/\text{min}$) is reported in the flow meter tab (C). Pressure sequencing is shown and controlled in the sequencer tab (D). Data recorded during mechanical testing is recorded and displayed real-time in the outer diameter, inlet pressure, outlet pressure, mean pressure, force, temperature, pH, and flow tab (E). A representative Pressure Diameter test of the vagina is displayed showing outer diameter as a function of time on the outer diameter tab.

Figure 6: Ultrasound Imaging. Ultrasound imaging of the murine reproductive organs. All images were taken using the ultrasound system on the short-axis-B mode. A representative image of the vagina at the unloaded length and pressure (A). Vaginal wall thickness was calculated in ImageJ. A vertical line was drawn along the depth scale (mm) to calibrate the number of pixels per μm . The polygon tool was used to trace the inner and outer diameter. Then transmural lines were drawn to calculate the thickness and averaged (B). This was performed 3 times. A representative image of the cervix at the unloaded length and pressure (C). Wall thickness was then calculated using Image J and the polygon tool in a similar manner to that of the vagina (D). Within the reproductive complex, the outer diameter is tracked at two different locations (E). Throughout the imaging process, the transducer is stabilized by a 3-D printed holder (F).

Figure 7: Representative results for vaginal testing. The representative mechanical testing results of the vaginal basal and passive protocols. With the data obtained by the DMT system, several mechanical relationships can be derived. A) Basal Pressure-Diameter, B) Passive Pressure-Diameter, C) Basal Force-Pressure, D) Passive Force-Pressure, E) Basal circumferential stress-circumferential stretch, F) Passive circumferential stress-circumferential stretch, G) Basal axial stress-circumferential stretch, H) Passive axial stress-circumferential stretch.

Figure 8: Representative results for cervical testing. The representative mechanical testing results of the cervical basal and passive protocols. With the data obtained by the DMT system, several mechanical relationships can be derived. A) Basal Pressure-Diameter, B) Passive Pressure-Diameter, C) Basal Force-Pressure, D) Passive Force-Pressure, E) Basal circumferential stress-circumferential stretch, F) Passive circumferential stress-circumferential stretch, G) Basal axial stress-circumferential stretch, H) Passive axial stress-circumferential stretch.

Table 1: Summary of information for scaling the mechanical testing methods for each organ. The unloaded pressure values were measured using catheterization techniques under anesthesia (4% isoflurane in 100% oxygen). A balloon catheter was utilized for the vaginal measurements and a 2F catheter for the cervix.

Table 2: The representative results for the physiological pressure measured within the vagina and cervix. Pressure was taken during both basal and passive conditions as well as for both circumferential and axial directions. All measurements provided are in units of kPa.

DISCUSSION:

The protocol provided in this article presents a method for determining the mechanical

properties of the murine vagina and cervix. The mechanical properties analyzed in this protocol include both the passive and basal tone conditions of the organs. Passive and basal tone conditions are induced by altering the biochemical environment in which the organ is submerged. For this protocol, the media involved in basal testing contains calcium. Testing the basal tone condition permits isolation of the smooth muscle cell mechanical contribution within the female reproductive organs^{54,55}. When performing passive mechanical testing, the media does not contain calcium. The lack of calcium inhibits the smooth muscle cells from contracting. This permits elucidation of other ECM components, such as collagen and elastic fibers, which largely dictate the passive mechanical properties. When combined with biochemical and histological analysis, these results permit elucidation of relationships between ECM microstructural composition and mechanical function. This then allows for delineation of the structural and mechanical mechanisms of pathologies relevant to women's reproductive health.

Previously, the vagina and cervix were tested uniaxially^{27,28}. The vagina and cervix, however, demonstrate anisotropic properties and experience multiaxial loading in vivo^{29,30}. Hence, pressure myograph systems used herein provide quantitative information on multiaxial loading that may aid in understanding the etiologies of reproductive pathologies, as well as the subsequent design of potential treatments. Further, pressure myography permits assessment of multiaxial properties while preserving the in vivo organ geometry and the native cell-matrix interaction⁵⁶. In vivo, the cells actively remodel the surrounding ECM in response to changes in biomechanical and biochemical cues⁵⁷⁻⁵⁹. The protocol used herein is advantageous as it permits monitoring of subsequent changes in bulk organ properties under physiologically relevant conditions. This aids in providing a platform to generate systematic datasets of multiaxial active and passive mechanical properties. Further, the data collected in these experiments may be leveraged to formulate and validate microstructurally-motivated nonlinear constitutive models to describe and predict the mechanical response of the female reproductive organs in healthy and pathological states^{16,60}.

An additional system component that was advantageous to the protocol was the use of ultrasound imaging to measure the thickness of the organ walls. The thickness is crucial information for calculating stress experienced while undergoing testing.

With any experimental set up, there are some limitations to this procedure. This protocol currently only considers the elastic response of the vagina and cervix and not the viscoelastic response. A potential method to mitigate this limitation in the future is to modify the existing protocol to include creep and stress relaxation assays⁶¹. A second limitation is assuming the organs are incompressible. Within this study, thickness was solely measured at the unloaded configuration, as motivated by prior studies that demonstrate nonpregnant murine tissue exhibits minimal changes in volume during osmotic loading⁶². Furthermore, additional studies have operated under the same assumption of incompressibility^{44,60,63}. Ideally, an ultrasound would be performed for the entirety of the experiment in order to remove the need for the incompressibility assumption and to better inform finite element models. A final limitation is the lack of quantified in vivo cervical pressure to inform the loading protocols. Literature suggests that cervical pressure in human women is 37 mmHg⁵³. Mice, however, may exhibit different

cervical pressure from that of humans. A difference in vaginal pressure was demonstrated between rodent models and human samples^{64,65}. Further studies are needed to quantify pressure in the non-pregnant murine cervix. Towards this end, intra-uterine pressure was recently reported throughout pregnancy⁴⁹.

The commercially available pressure myograph system utilized in this procedure measures the force properties of elastic, hollow organs. This protocol is easily adaptable to other various organs and tissues by modifying the chemical additives in the bath, cannula size, and suture thickness.

ACKNOWLEDGMENTS:

The work was funded by NSF CAREER award grant #1751050.

DISCLOSURES:

None.

REFERENCES

- 1 Capone, D. et al. Evaluating Residual Strain Throughout the Murine Female Reproductive System. *Journal of Biomechanics*. **82**, 299-306, doi:10.1016/j.jbiomech.2018.11.001 (2019).
- 2 Danforth, D. The fibrous nature of the human cervix, and its relation to the isthmic segment in gravid and nongravid uteri. *American Journal of Obstetrics and Gynecology*. **53** (4), 541-560 (1947).
- 3 Hughesdon, P. The fibromuscular structure of the cervix and its changes during pregnancy and labour. *Journal of Obstetrics and Gynecology of the British Commonwealth*. **59**, 763-776 (1952).
- 4 Bryman, I., Norstrom, A., Lindblo, B. Influence of neurohypophyseal hormones on human cervical smooth muscle cell contractility in vitro. *Obstetrics and Gynecology*. **75** (2), 240-243 (1990).
- 5 Joy, V. et al. A New Paradigm for the Role of Smooth Muscle Cells in the Human Cervix. *Obstetrics*. **215** (4), 478.e471-478.e411 (2016).
- 6 Xu, X., Akgul, Y., Mahendroo, M., Jerschow, A. Ex vivo assessment of mouse cervical remodeling through pregnancy via Na (23) MRS. *NMR Biomedical*. **23** (8), 907-912 (2014).
- 7 Leppert, P. Anatomy and Physiology of cervical ripening. *Clinical Obstetrics and Gynecology*. **2000** (43), 433-439 (1995).
- 8 Schlembach, D. et al. Cervical ripening and insufficiency: from biochemical and molecular studies to in vivo clinical examination. *European Journal of Obstetrics, Gynecology, and Reproductive Biology*. **144**, S70-S79 (2000).
- 9 Stoka, K. et al. Effects of Increased Arterial Stiffness on Atherosclerotic Plaque Amounts. *Journal of Biomechanical Engineering*. **140** (5) (2018).
- 10 Mohram, D., Heller, L. in *Cardiovascular Physiology* Ch. 7, (The McGraw-Hill Companies, 2006).
- 11 Yoshida, K. et al. Quantitative Evaluation of Collagen Crosslinks and Corresponding Tensile Mechanical Properties in Mouse Cervical Tissue during Normal Pregnancy. *PLoS One*. **9**, e112391 (2014).

694 12 Mahendroo, M. Cervical remodeling in term and preterm birth: insight from an animal
695 model. *Society for Reproduction and Fertility*. **143** (4), 429-438 (2012).

696 13 Elovitz, M., Miranlini, C. Can medroxyprogesterone acetate alter Toll-like receptor
697 expression in a mouse model of intrauterine inflammation? *American Journal of*
698 *Obstetrics and Gynecology*. **193** (3), 1149-1155 (2005).

699 14 Ripperda, C. et al. Vaginal estrogen: a dual-edged sword in postoperative healing of the
700 vaginal wall. *North American Menopause Society*. **24** (7), 838-849 (2017).

701 15 Nelson, J., Felicio, P., Randall, K., Sims, C., Finch, E. A Longitudinal Study of Estrous Cyclicity
702 in Aging C57/6J Mice: Cycle, Frequency, Length, and Vaginal Cytology. *Biology of*
703 *Reproduction*. **27** (2), 327-339 (1982).

704 16 Ferruzzi, J., Collins, M., Yeh, A., Humphrey, J. Mechanical assessment of elastin integrity
705 in fibrillin-1-deficient carotid arteries: implications for Marfan Syndrome. *Cardiovascular*
706 *Research*. **92** (2), 287-295 (2011).

707 17 Mariko, B. et al. Fibrillin-1 genetic deficiency leads to pathological ageing of arteries in
708 mice. *The Journal of Pathology*. **224** (1), 33-44 (2011).

709 18 Rahn, D., Ruff, M., Brown, S., Tibbals, H., Word, R. Biomechanical Properties of The Vaginal
710 Wall: Effect of Pregnancy, Elastic Fiber Deficiency, and Pelvic Organ Prolapse. *American*
711 *Urogynecological Society*. **198** (5), 590.e1-590.e6 (2009).

712 19 Caulk, A., Nepiyushchikh, Z., Shaw, R., Dixon, B., Gleason, R. Quantification of the passive
713 and active biaxial mechanical behavior and microstructural organization of rat thoracic
714 ducts. *Royal Society Interface*. **12** (108), 20150280 (2015).

715 20 Amin, M., Le, V., Wagenseil, J. Mechanical Testing of Mouse Carotid Arteries: from
716 Newborn to Adult. *Journal of Visualized Experiments*. (60), e3733 (2012).

717 21 Sokolis, D., Sassani, S., Kritharis, E., Tsangaris, S. Differential histomechanical response of
718 carotid artery in relation to species and region: mathematical description accounting for
719 elastin and collagen anisotropy. *Medical and Biological Engineering and Computing*. **49**
720 (8), 867-879 (2011).

721 22 Kim, J., Baek, S. Circumferential variations of the mechanical behavior of the porcine
722 thoracic aorta during the inflation test. *Journal of Biomechanics*. **44** (10), 1941-1947
723 (2011).

724 23 Faury, G. et al. Developmental adaptation of the mouse cardiovascular system to elastin
725 haploinsufficiency. *Journal of Clinical Investigation*. **11** (9), 1419-1428 (2003).

726 24 Naito, Y. et al. Beyond Burst Pressure: Initial Evaluation of the Natural History of the
727 Biaxial Mechanical Properties of Tissue-Engineered Vascular Grafts in the Venous
728 Circulation Using a Murine Model. *Tissue Engineering*. **20**, 346-355 (2014).

729 25 Sommer, G. et al. Multiaxial mechanical response and constitutive modeling of esophageal
730 tissues: Impact on esophageal tissue engineering. *Acta Biomaterialia*. **9** (12), 9379-9391
731 (2013).

732 26 Sokolis, D., Orfanidis, I., Peroulis, M. Biomechanical testing and material characterization
733 for the rat large intestine: regional dependence of material parameters. *Physiological*
734 *Measurement*. **32** (12) 1969-1982 (2011).

735 27 Martins, P. et al. Prediction of Nonlinear Elastic Behavior of Vaginal Tissue: Experimental
736 Results and Model Formation. *Computational Methods of Biomechanics and Biomedical*
737 *Engineering*. **13** (3), 317-337 (2010).

738 28 Feola, A. et al. Deterioration in Biomechanical Properties of the Vagina Following
739 Implantation of a High-stiffness Prolapse Mesh. *BJOG: An International Journal of*
740 *Obstetrics and Gynaecology*. **120** (2), 224-232 (2012).

741 29 Huntington, A., Rizzuto, E., Abramowitch, S., Prete, Z., De Vita, R. Anisotropy of the Passive
742 and Active Rat Vagina Under Biaxial Loading. *Annals of Biomedical Engineering*. **47**, 272-
743 281 (2018).

744 30 Tokar, S., Feola, A., Moalli, P., Abramowitch, S. Characterizing the Biaxial Mechanical
745 Properties of Vaginal Maternal Adaptations During Pregnancy. *ASME 2010 Summer*
746 *Bioengineering Conference, Parts A and B*. 689-690 (2010).

747 31 Feloa, A. et al. Impact of Pregnancy and Vaginal Delivery on the Passive and Active
748 Mechanics of the Rat Vagina. *Annals of Biomedical Engineering*. **39** (1), 549-558 (2010).

749 32 Baah-Dwomoh, A., Alperin, M., Cook, M., De Vita, R. Mechanical Analysis of the
750 Uterosacral Ligament: Swine vs Human. *Annual Biomedical Engineering*. **46** (12), 2036-
751 2047 (2018).

752 33 Champlin, A. Determining the Stage of the Estrous Cycle in the Mouse by the Appearance.
753 *Biology of Reproduction*. **8** (4), 491-494 (1973).

754 34 Byers, S., Wiles, M., Dunn, S., Taft, R. Mouse Estrous Cycle Identification Tool and Images.
755 *PLoS One*. **7** (4), e35538 (2012).

756 35 McLean, A. Performing Vaginal Lavage, Crystal Violet Staining and Vaginal Cytological
757 Evaluation for Mouse Estrous Cycle Staging Identification. *Journal of Visualized*
758 *Experiments*. **67**, e4389 (2012).

759 36 Bugg, G., Riley, M., Johnston, T., Baker, P., Taggart, M. Hypoxic inhibition of human
760 myometrial contractions in vitro: implications for the regulation of parturition. *European*
761 *Journal of Clinical Investigation*. **36** (2), 133-140 (2006).

762 37 Taggart, M., Wray, S. Hypoxia and smooth muscle function: key regulatory events during
763 metabolic stress. *Journal of Physiology*. **509**, 315-325 (1998).

764 38 Yoo, K. et al. The effects of volatile anesthetics on spontaneous contractility of isolated
765 human pregnant uterine muscle: a comparison among sevoflurane, desflurane,
766 isoflurane, and halothane. *Anesthesia and Analgesia*. **103** (2), 443-447 (2006).

767 39 de Souza, L. et al. Effects of redox disturbances on intentional contractile reactivity in rats
768 fed with a hypercaloric diet. *Oxidative Medicine and Cellular Longevity*. **2018**, 6364821
769 (2018).

770 40 Jaue, D., Ma, Z., Lee, S. Cardiac muscarinic receptor function in rats with cirrhotic
771 cardiomyopathy. *Hepatology*. **25**, 1361-1365 (1997).

772 41 Xu, Q., Shaffer, E. The potential site of impaired gallbladder contractility in an animal
773 mode of cholesterol gallstone disease. *Gastroenterology*. **110** (1), 251-257 (1996).

774 42 Rodriguez, U. et al. Effects of blast induced Neurotrauma on pressurized rodent middle
775 cerebral arteries. *Journal of Visualized Experimentals*. (146), e58792 (2019).

776 43 Rubod, C., Boukerrou, M., Brieu, M., Dubois, P., Cosson, M. Biomechanical Properties of
777 Vaginal Tissue Part 1: New Experimental Protocol. *Journal of Urology*. **178**, 320-325
778 (2007).

779 44 Robison, K., Conway, C., Desrosiers, L., Knoepp, L., Miller, K. Biaxial Mechanical
780 Assessment of the Murine Vaginal Wall Using Extension-Inflation Testing. *Journal of*
781 *Biomechanical Engineering*. **139** (10), 104504 (2017).

782 45 Van loon, P. Length-Force and Volume-Pressure Relationships of Arteries. *Biorheology*. **14**
783 (4), 181-201 (1977).

784 46 Fernandez, M. et al. Investigating the Mechanical Function of the Cervix During Pregnancy
785 using Finite Element Models Derived from High Resolution 3D MRI. *Computational*
786 *Methods Biomechanical and Biomedical Engineering*. **19** (4), 404-417 (2015).

787 47 House, M., Socrate, S. The Cervix as a Biomechanical Structure. *Ultrasound Obstetric*
788 *Gynecology*. **28** (6), 745-749 (2006).

789 48 Martins, P. et al. Biomechanical Properties of Vaginal Tissue in Women with Pelvic Organ
790 Prolapse. *Gynecologic and Obstetrics Investigation*. **75**, 85-92 (2013).

791 49 Rada, C., Pierce, S., Grotegut, C., England, S. Intrauterine Telemetry to Measure Mouse
792 Contractile Pressure In vivo *Journal of Visualized Experiments*. (98), e52541 (2015).

793 50 Lumsden, M. A., Baird, D. T. Intra-uterine pressure in dysmenorrhea. *Acta Obstetricia et*
794 *Gynecologica Scandinavica*. **64** (2), 183-186 (1985).

795 51 Milsom, I., Andersch, B., Sundell, G. The Effect of Flurbiprofen and Naproxen Sodium On
796 Intra-Uterine Pressure and Menstrual Pain in Patients With Primary Dysmennorrhea. *Acta*
797 *Obstetricia et Gynecologica Scandinavica*. **67** (8), 711-716 (1988).

798 52 Park, K. et al. Vasculogenic female sexual dysfunction: the hemodynamic basis for vaginal
799 engorgement insufficiency and clitoral erectile insufficiency. *International Journal of*
800 *Impotence Journal*. **9** (1), 27-37 (1997).

801 53 Bulletti, C. et al. Uterine Contractility During Menstrual Cycle. *Human Reproduction*. **15**,
802 81-89 (2000).

803 54 Kim, N. N. et al. Effects of Ovariectomy and Steroid Hormones on Vaginal Smooth Muscle
804 Contractility. *International Journal of Impotence Research*. **16**, 43-50 (2004).

805 55 Giraldi, A. et al. Morphological and Functional Characterization of a Rat Vaginal Smooth
806 Muscle Sphincter. *International Journal of Impotence Research*. **14**, 271-282 (2002).

807 56 Gleason, R., Gray, S. P., Wilson, E., Humphrey, J. A Multiaxial Computer-Controlled Organ
808 Culture and Biomechanical Device for Mouse Carotid Arteries. *Journal of Biomechanical*
809 *Engineering*. **126** (6), 787-795 (2005).

810 57 Swartz, M., Tscumperlin, D., Kamm, R., Drazen, J. Mechanical Stress is Communicated
811 Between Different Cell Types to Elicit Matrix Remodeling. *Proceedings of the National*
812 *Academy of Sciences of the United States of America*. **98** (11) 6180-6185 (2001).

813 58 Rachev, A. Remodeling of Arteries in Response to Changes in their Mechanical
814 Environment. *Biomechanics of Soft Tissue in Cardiovascular Systems*. **441**, 221-271 (2003).

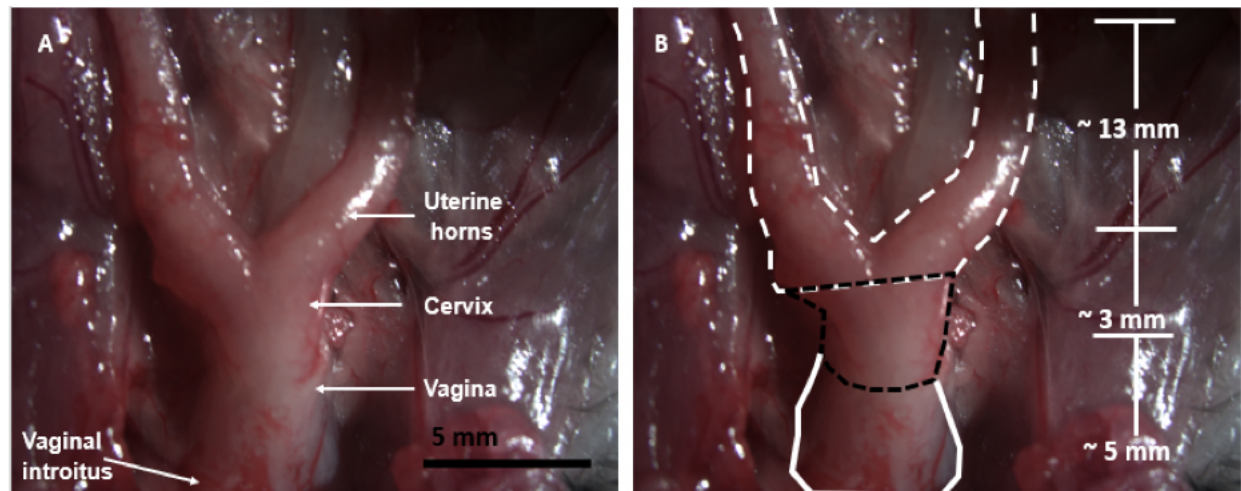
815 59 Lee, E. J., Holmes, J., Costa, K. Remodeling of Engineered Tissue Anisotropy in Response
816 to Altered Loading Conditions. *Annals of Biomedical Engineering*. **36** (8), 1322-1334
817 (2008).

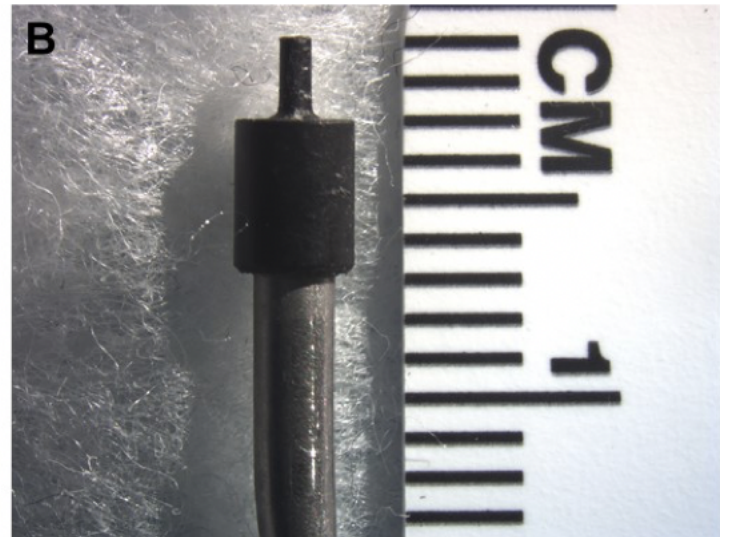
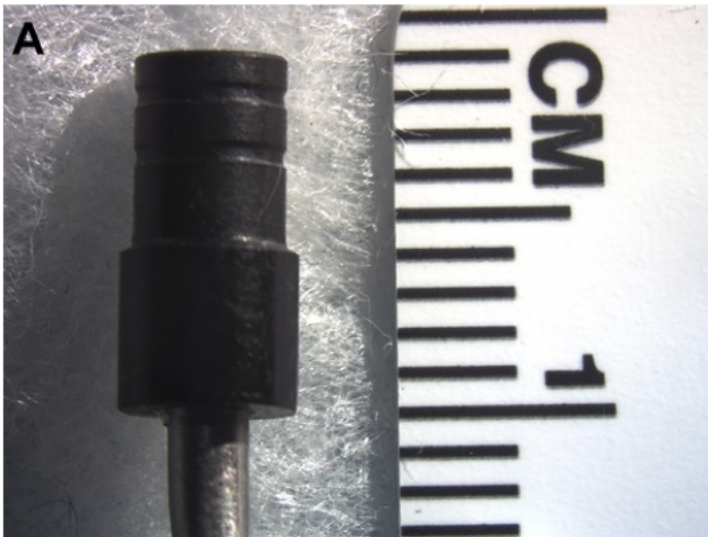
818 60 Akintunde, A. et al. Effects of Elastase Digestion on the Murine Vaginal Wall Biaxial
819 Mechanical Response. *Journal of Biomechanical Engineering*. **141** (2), 021011 (2018).

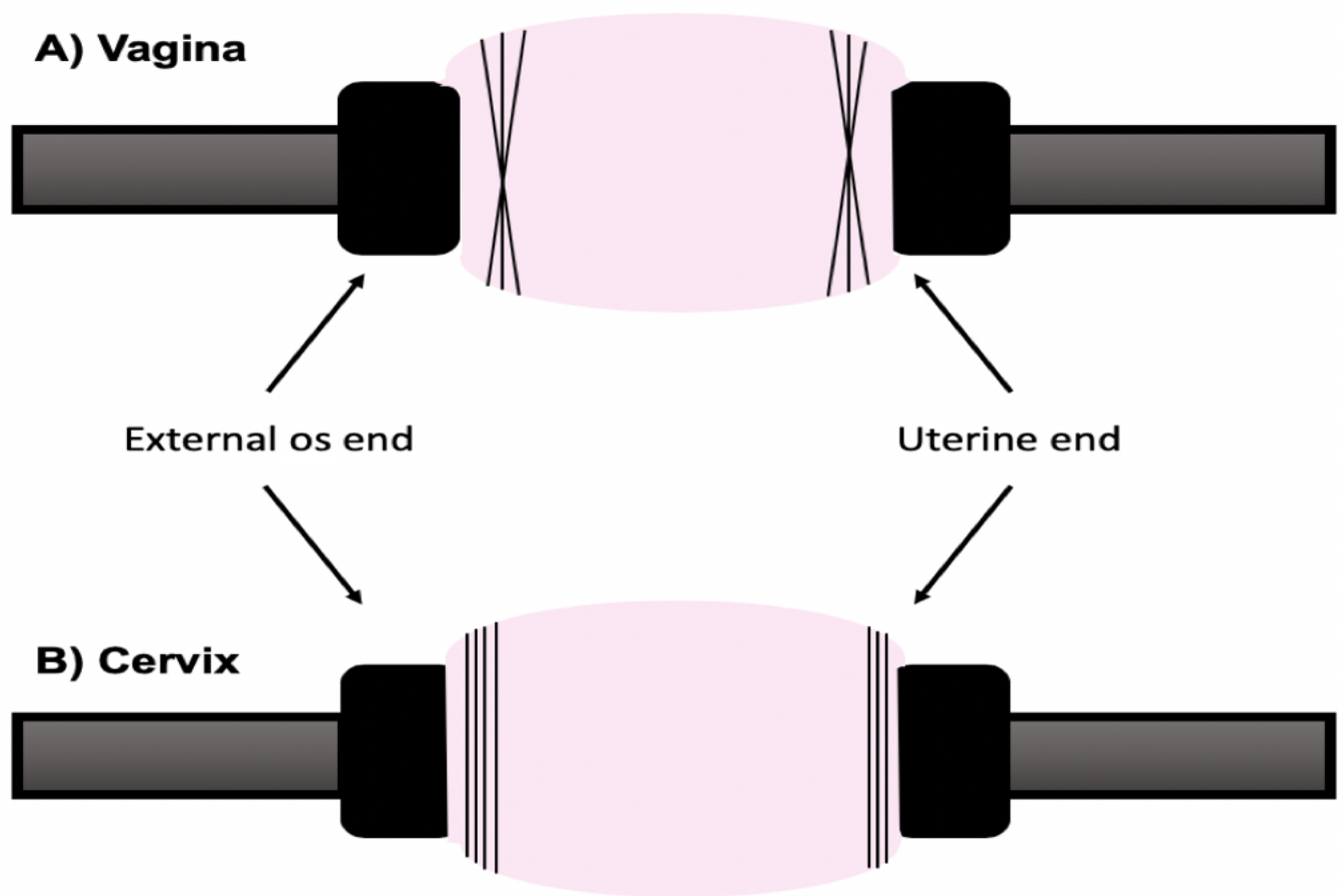
820 61 Griffin, M., Premakumar, Y., Seifalian, A., Butler, P., Szarko, M. Biomechanical
821 Characterization of Human Soft Tissues Using Indentation and Tensile Testing. *Journal of*
822 *Visualized Experiments*. (118), e54872 (2016).

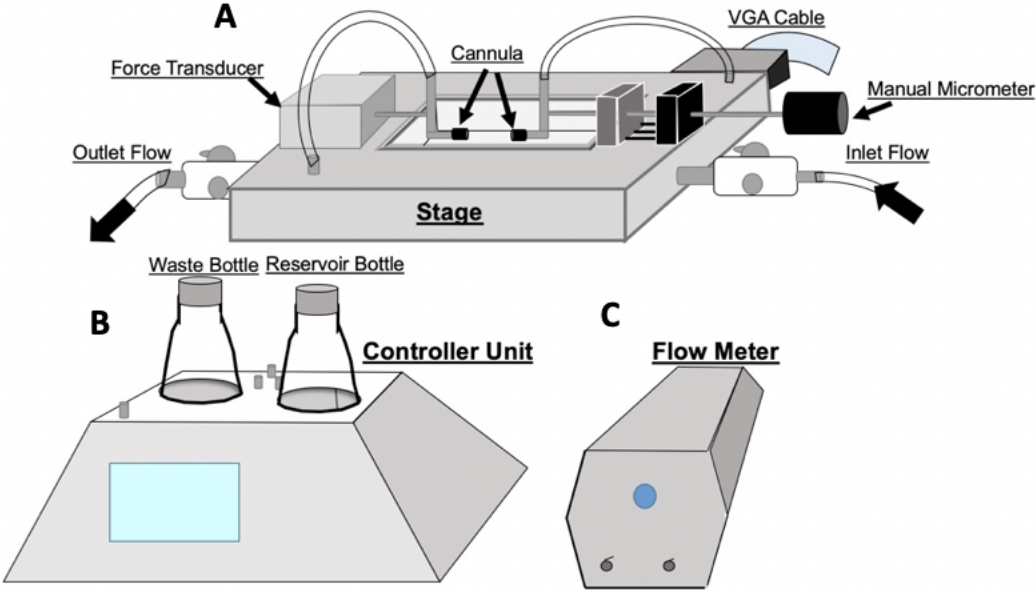
823 62 Myers, K., Socrate, S., Paskaleva, A., House, M. A Study of the Anisotropy and
824 Tension/Compression Behavior of Human Cervical Tissue. *Journal of Biomechanical*
825 *Engineering*. **132** (2), 021003 (2010).

826 63 Murtada, S., Ferruzzi, J., Yanagisawa, H., Humphrey, J. Reduced Biaxial Contractility in the
827 Descending Thoracic Aorta of Fibulin-5 Deficient Mice. *Journal of Biomechanical*
828 *Engineering*. **138** (5), 051008 (2016).
829 64 Berkley, K., McAllister, S., Accius, B., Winnard, K. Endometriosis-induced vaginal
830 hyperalgesia in the rat: effect of estropause, ovariectomy, and estradiol replacement.
831 *Pain*. **132**, s150-s159 (2007).
832 65 van der Walt, L., Bo, K., Hanerkom., Rienhardt, G. Ethnic Differences in pelvic floor muscle
833 strength and endurance in South African women. *International Urogynecology Journal*.
834 **25** (6), 799-805 (2014).
835
836
837

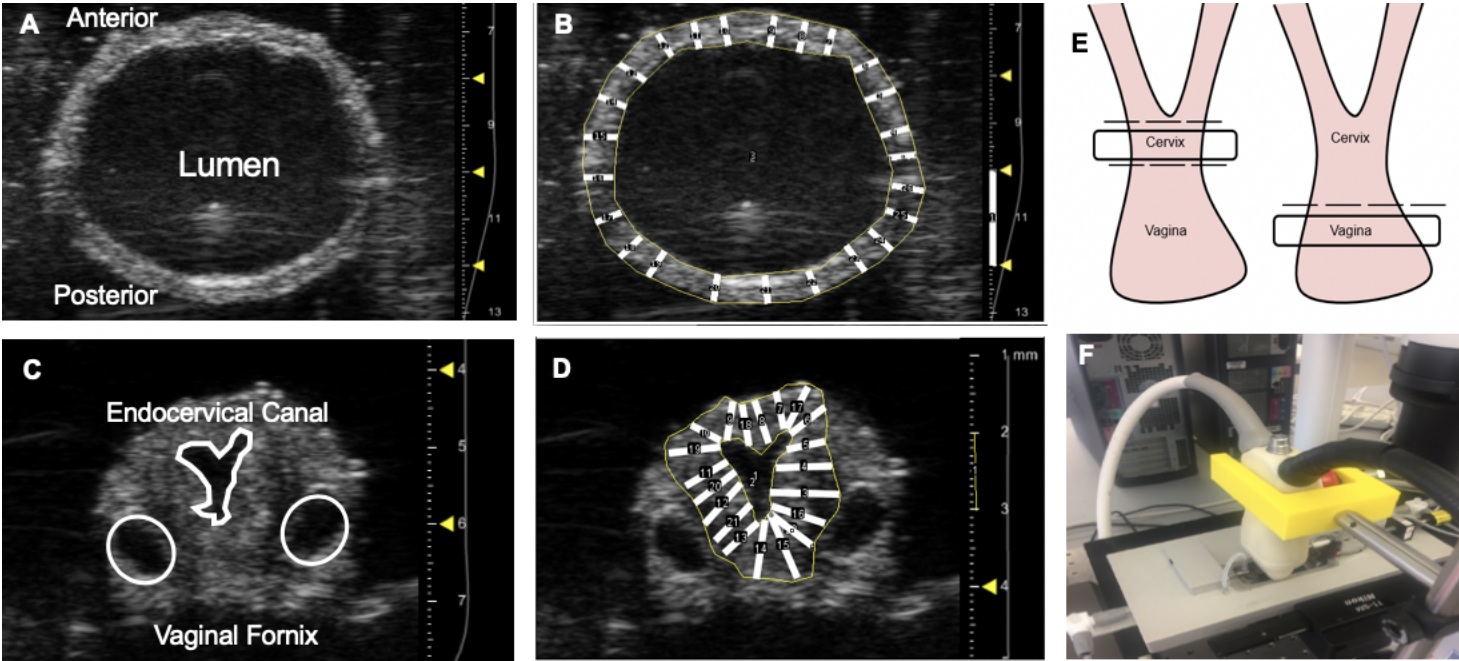


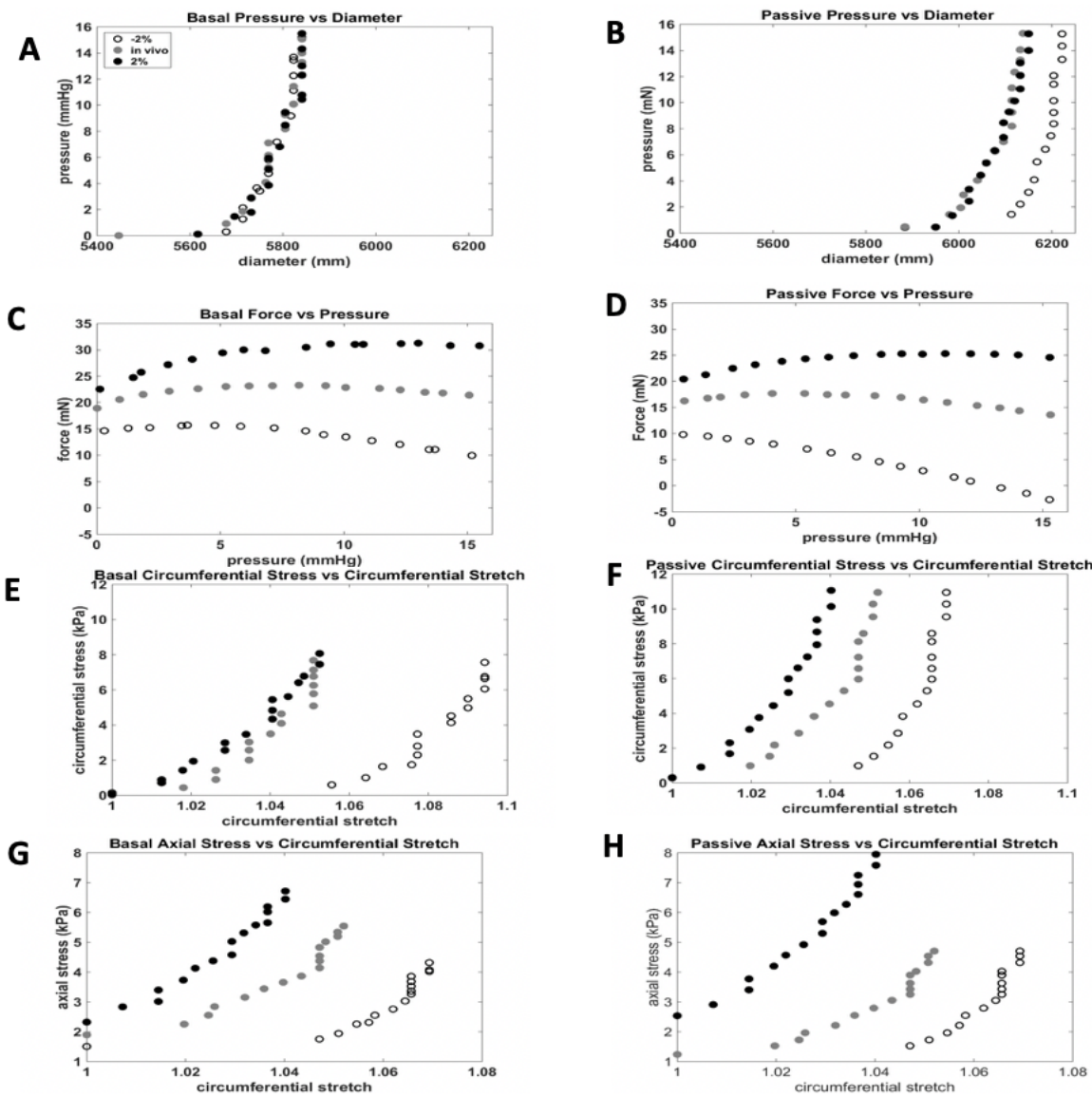












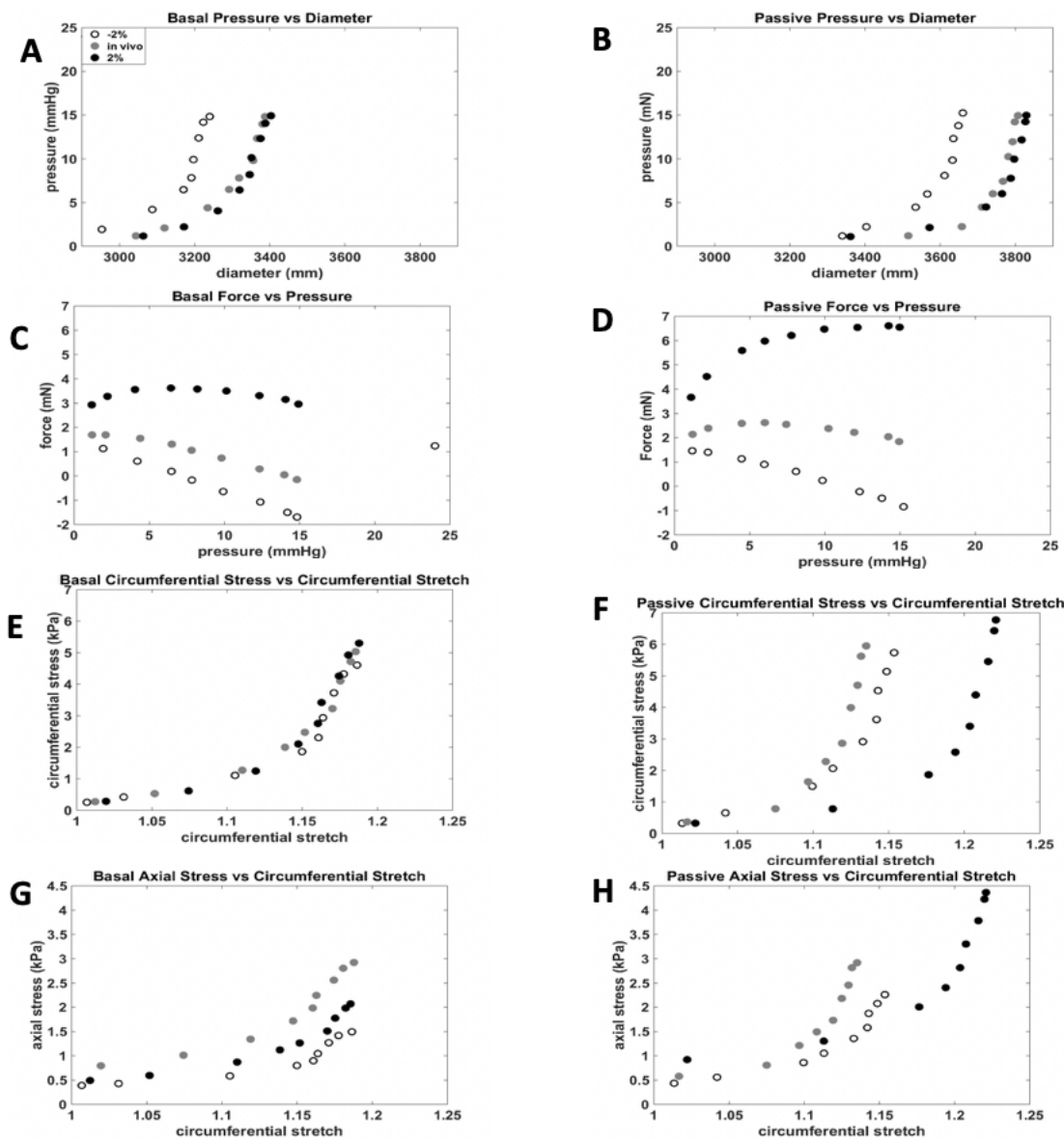


Table 1

	In Vivo Pressure	Maximum Pressure	1/3 Max Pressure	2/3 Max Pressure	Axial Stretch	Cannula Size	Recommended number of sutures
Vagina	7 mmHg	15 mmHg	5 mmHg	10 mmHg	-2%, in vivo, +2%	3.75 mm	3-- in an "X"
						0.75 mm for uterine end	3 horizontal sutures on the uterine end
Cervix	10 mmHg	200 mmHg	66 mmHg	133 mmHg	-2%, in vivo, +2%	3.75 mm for vaginal end	4 sutures on the vaginal external os

	Vagina	Cervix
Basal		
Circumferential		
(kPa)	127.94	188
Basal		
Axial (kPa)	56.8	75.44
Passive		
Circumferential		
(kPa)	246.03	61.26
Passive		
Axial (kPa)	112.74	19.26

Name of Material/ Equipment	Company	Catalog Number	Comments/Description
2F catheter	Millar	SPR-320	catheter to measure cervical pressure
6-0 Suture	Fine Science Tools	18020-60	larger suture ties
CaCl ₂ (anhydrous)	VWR	97062-590	HBSS concentration: 140 mg/ mL
CaCl ₂ -2H ₂ O	Fischer chemical	BDH9224-1KG	KRB concentration: 3.68 g/L
Dextrose (D-glucose)	VWR	101172-434	HBSS concentration: 1000 mg/mL KRB concentration: 19.8 g/L
Dumont #5/45 Forceps	Fine Science Tools	11251-35	curved forceps
Dumont SS Forceps	Fine Science Tools	11203-25	straight forceps
Eclipse	Nikon	E200	microscope used for imaging
Flow meter	Danish MyoTechnologies	161FM	flow meter within the testing apparatus
Force Transducer - 110P	Danish MyoTechnologies	100079	force transducer
ImageJ	SciJava	ImageJ1	used to measure volume
Instrument Cases	Fine Science Tools	20830-00	casing to hold dissection tools
KCl	Fisher Chemical	97061-566	HBSS concentration: 400 mg/ mL KRB concentration: 3.5 g/L
KH ₂ PO ₄	G-Biosciences	71003-454	HBSS concentration: 60 mg/ mL
MgCl ₂	VWR	97064-150	KRB concentration: 1.14 g/L
MgCl ₂ -6H ₂ O	VWR	BDH9244-500G	HBSS concentration: 100 mg/ mL
MgSO ₄ -7H ₂ O	VWR	97062-134	HBSS concentration: 48 mg/ mL
Mircosoft excel	Microsoft	6278402	program used for spreadsheet
Na ₂ HPO ₄ (dibasic anhydrous)	VWR	97061-588	HBSS concentration: 48 mg/mL KRB concentration: 1.44 g/L
NaCl	VWR	97061-274	HBSS concentration: 8000 mg/mL KRB concentration: 70.1 g/L
NaHCO ₃	VWR	97062-460	HBSS concentration: 350 mg/ mL KRB concentration: 21.0 g/L
Pressure myograph systems	Danish MyoTechnologies	110P and 120CP	Pressure myograph system: program, cannulation device, and controller unit
Pressure Transducer	Danish MyoTechnologies	100106	pressure transducer

Student Dumont #5 Forceps	Fine Science Tools	91150-20	straight forceps
Student Vannas Spring Scissors	Fine Science Tools	91500-09	micro-scissors
Tissue dye	Bradley Products	1101-3	ink to measure in vivo stretch
Ultrasound transducer	FujiFilm Visual Sonics	LZ-550	ultrasound transducer used; 256 elements, 40 MHz center frequency
VEVO2100	FujiFilm Visual Sonics	VS-20035	ultrasound used for imaging
Wagner Scissors	Fine Science Tools	14069-12	larger scissors

ARTICLE AND VIDEO LICENSE AGREEMENT

Title of Article:

Biaxial Basal Tone and Passive Testing of the Murine Reproductive System Using a Pressure Myograph System

Author(s):

Shelby E. White, Cassandra K. Conway, Gabrielle L. Clark, Dylan J. Lawrence, Carolyn L. Bayer, Kristin S. Miller

Item 1: The

Author elects to have the Materials be made available (as described at <http://www.jove.com/publish>) via:



Standard Access



Open Access

Item 2: Please select one of the following items:



The Author is **NOT** a United States government employee.



The Author is a United States government employee and the Materials were prepared in the course of his or her duties as a United States government employee. ☐ The Author is a United States government employee but the Materials were NOT prepared in the course of his or her duties as a United States government employee.

ARTICLE AND VIDEO LICENSE AGREEMENT

1. **Defined Terms.** As used in this Article and Video License Agreement, the following terms shall have the following meanings: "**Agreement**" means this Article and Video License Agreement; "**Article**" means the article specified on the last page of this Agreement, including any associated materials such as texts, figures, tables, artwork, abstracts, or summaries contained therein; "**Author**" means the author who is a signatory to this Agreement; "**Collective Work**" means a work, such as a periodical issue, anthology or encyclopedia, in which the Materials in their entirety in unmodified form, along with a number of other contributions, constituting separate and independent works in themselves, are assembled into a collective whole; "**CRC License**" means the Creative Commons AttributionNon Commercial-No Derivs 3.0 Unported Agreement, the terms and conditions of which can be found at: <http://creativecommons.org/licenses/by-ncnd/3.0/legalcode>; "**Derivative Work**" means a work based upon the Materials or upon the Materials and other preexisting works, such as a translation, musical arrangement, dramatization, fictionalization, motion picture version, sound recording, art reproduction, abridgment, condensation, or any other form in which the Materials may be recast, transformed, or adapted; "**Institution**" means the institution, listed on the last page of this Agreement, by which the Author was employed at the time of the creation of the Materials; "**JoVE**" means MyJoVE Corporation, a Massachusetts corporation and the

publisher of The Journal of Visualized Experiments; "**Materials**" means the Article and / or the Video; "**Parties**" means the Author and JoVE; "**Video**" means any video(s) made by the Author, alone or in conjunction with any other parties, or by JoVE or its affiliates or agents, individually or in collaboration with the Author or any other parties, incorporating all or any portion of the Article, and in which the Author may or may not appear.

2. **Background.** The Author, who is the author of the Article, in order to ensure the dissemination and protection of the Article, desires to have the JoVE publish the Article and create and transmit videos based on the Article. In furtherance of such goals, the Parties desire to memorialize in this Agreement the respective rights of each Party in and to the Article and the Video.

3. **Grant of Rights in Article.** In consideration of JoVE agreeing to publish the Article, the Author hereby grants to JoVE, subject to Sections 4 and 7 below, the exclusive, royalty-free, perpetual (for the full term of copyright in the Article, including any extensions thereto) license (a) to publish, reproduce, distribute, display and store the Article in all forms, formats and media whether now known or hereafter developed (including without limitation in print, digital and electronic form) throughout the world, (b) to translate the Article into other languages, create adaptations, summaries or extracts of the Article or other Derivative Works (including, without limitation, the Video) or Collective Works based on all or any portion of the Article

and exercise all of the rights set forth in (a) above in such translations, adaptations, summaries, extracts, Derivative Works or Collective Works and(c) to license others to do any or all of the above. The foregoing rights may be exercised in all media and formats, whether now known or hereafter devised, and include the right to make such modifications as are technically necessary to exercise the rights in other media and formats. If the "Open Access" box has been checked in **Item 1** above, JoVE and the Author hereby grant to the public all such rights in the Article as provided in, but subject to all limitations and requirements set forth in, the CRC License.

4. **Retention of Rights in Article.** Notwithstanding the exclusive license granted to JoVE in **Section 3** above, the Author shall, with respect to the Article, retain the nonexclusive right to use all or part of the Article for the noncommercial purpose of giving lectures, presentations or teaching classes, and to post a copy of the Article on the Institution's website or the Author's personal website, in each case provided that a link to the Article on the JoVE website is provided and notice of JoVE's copyright in the Article is included. All non-copyright intellectual property rights in and to the Article, such as patent rights, shall remain with the Author.

5. **Grant of Rights in Video – Standard Access.** This **Section 5** applies if the "Standard Access" box has been checked in **Item 1** above or if no box has been checked in **Item 1** above. In consideration of JoVE agreeing to produce, display or otherwise assist with the Video, the Author hereby acknowledges and agrees that, Subject to **Section 7** below, JoVE is and shall be the sole and exclusive owner of all rights of any nature, including, without limitation, all copyrights, in and to the Video. To the extent that, by law, the Author is deemed, now or at any time in the future, to have any rights of any nature in or to the Video, the Author hereby disclaims all such rights and transfers all such rights to JoVE.

6. **Grant of Rights in Video – Open Access.** This **Section 6** applies only if the "Open Access" box has been checked in **Item 1** above. In consideration of JoVE agreeing to produce, display or otherwise assist with the Video, the Author hereby grants to JoVE, subject to **Section 7** below, the exclusive, royalty-free, perpetual (for the full term of copyright in the Article, including any extensions thereto) license (a) to publish, reproduce, distribute, display and store the Video in all forms, formats and media whether now known or hereafter developed (including without limitation in print, digital and electronic form) throughout the world, (b) to translate the Video into other languages, create adaptations, summaries or extracts of the Video or other Derivative Works or Collective Works based on all or any portion of the Video and exercise all of the rights set forth in (a) above in such translations, adaptations, summaries, extracts, Derivative Works or Collective Works and (c) to license others to do any or all of the above. The foregoing rights may be exercised in all media and formats, whether now known or hereafter devised, and include the

right to make such modifications as are technically necessary to exercise the rights in other media and formats. For any Video to which this **Section 6** is applicable, JoVE and the Author hereby grant to the public all such rights in the Video as provided in, but subject to all limitations and requirements set forth in, the CRC License.

7. **Government Employees.** If the Author is a United States government employee and the Article was prepared in the course of his or her duties as a United States government employee, as indicated in **Item 2** above, and any of the licenses or grants granted by the Author hereunder exceed the scope of the 17 U.S.C. 403, then the rights granted hereunder shall be limited to the maximum rights permitted under such statute. In such case, all provisions contained herein that are not in conflict with such statute shall remain in full force and effect, and all provisions contained herein that do so conflict shall be deemed to be amended so as to provide to JoVE the maximum rights permissible within such statute.

8. **Protection of the Work.** The Author(s) authorize JoVE to take steps in the Author(s) name and on their behalf if JoVE believes some third party could be infringing or might infringe the copyright of either the Author's Article and/or Video.

9. **Likeness, Privacy, Personality.** The Author hereby grants JoVE the right to use the Author's name, voice, likeness, picture, photograph, image, biography and performance in any way, commercial or otherwise, in connection with the Materials and the sale, promotion and distribution thereof. The Author hereby waives any and all rights he or she may have, relating to his or her appearance in the Video or otherwise relating to the Materials, under all applicable privacy, likeness, personality or similar laws. 10. **Author Warranties.** The Author represents and warrants that the Article is original, that it has not been published, that the copyright interest is owned by the Author (or, if more than one author is listed at the beginning of this Agreement, by such authors collectively) and has not been assigned, licensed, or otherwise transferred to any other party. The Author represents and warrants that the author(s) listed at the top of this Agreement are the only authors of the Materials. If more than one author is listed at the top of this Agreement and if any such author has not entered into a separate Article and Video License Agreement with JoVE relating to the Materials, the Author represents and warrants that the Author has been authorized by each of the other such authors to execute this Agreement on his or her behalf and to bind him or her with respect to the terms of this Agreement as if each of them had been a party hereto as an Author. The Author warrants that the use, reproduction, distribution, public or private performance or display, and/or modification of all or any portion of the Materials does not and will not violate, infringe and/or misappropriate the patent, trademark, intellectual property or other rights of any third party. The Author represents and warrants that it has and will continue to comply with all government, institutional and other

ARTICLE AND VIDEO LICENSE AGREEMENT

regulations, including, without limitation all institutional, laboratory, hospital, ethical, human and animal treatment, privacy, and all other rules, regulations, laws, procedures or guidelines, applicable to the Materials, and that all research involving human and animal subjects has been approved by the Author's relevant institutional review board.

11. JoVE Discretion. If the Author requests the assistance of JoVE in producing the Video in the Author's facility, the Author shall ensure that the presence of JoVE employees, agents or independent contractors is in accordance with the relevant regulations of the Author's institution. If more than one author is listed at the beginning of this Agreement, JoVE may, in its sole discretion, elect not take any action with respect to the Article until such time as it has received complete, executed Article and Video License Agreements from each such author. JoVE reserves the right, in its absolute and sole discretion and without giving any reason therefore, to accept or decline any work submitted to JoVE. JoVE and its employees, agents and independent contractors shall have full, unfettered access to the facilities of the Author or of the Author's institution as necessary to make the Video, whether actually published or not. JoVE has sole discretion as to the method of making and publishing the Materials, including, without limitation, to all decisions regarding editing, lighting, filming, timing of publication, if any, length, quality, content and the like.

12. Indemnification. The Author agrees to indemnify JoVE and/or its successors and assigns from and against any and all claims, costs, and expenses, including attorney's fees, arising out of any breach of any warranty or other representations contained herein. The Author further agrees to indemnify and hold harmless JoVE from and against any and all claims, costs, and expenses, including attorney's fees, resulting from the breach by the Author of any representation or warranty contained herein or from allegations or instances of violation of intellectual property rights, damage to the Author's or the Author's institution's facilities, fraud, libel, defamation, research, equipment, experiments, property damage, personal injury, violations of

institutional, laboratory, hospital, ethical, human and animal treatment, privacy or other rules, regulations, laws, procedures or guidelines, liabilities and other losses or damages related in any way to the submission of work to JoVE, making of videos by JoVE, or publication in JoVE or elsewhere by JoVE. The Author shall be responsible for, and shall hold JoVE harmless from, damages caused by lack of sterilization, lack of cleanliness or by contamination due to the making of a video by JoVE its employees, agents or independent contractors. All sterilization, cleanliness or decontamination procedures shall be solely the responsibility of the Author and shall be undertaken at the Author's expense. All indemnifications provided herein shall include JoVE's attorney's fees and costs related to said losses or damages. Such indemnification and holding harmless shall include such losses or damages incurred by, or in connection with, acts or omissions of JoVE, its employees, agents or independent contractors. **13. Fees.** To cover the cost incurred for publication, JoVE must receive payment before production and publication of the Materials. Payment is due in 21 days of invoice. Should the Materials not be published due to an editorial or production decision, these funds will be returned to the Author. Withdrawal by the Author of any submitted Materials after final peer review approval will result in a US\$1,200 fee to cover pre-production expenses incurred by JoVE. If payment is not received by the completion of filming, production and publication of the Materials will be suspended until payment is received. **14. Transfer, Governing Law.** This Agreement may be assigned by JoVE and shall inure to the benefits of any of JoVE's successors and assignees. This Agreement shall be governed and construed by the internal laws of the Commonwealth of Massachusetts without giving effect to any conflict of law provision thereunder. This Agreement may be executed in counterparts, each of which shall be deemed an original, but all of which together shall be deemed to me one and the same agreement. A signed copy of this Agreement delivered by facsimile, e-mail or other means of electronic transmission shall be deemed to have the same legal effect as delivery of an original signed copy of this Agreement.

A signed copy of this document must be sent with all new submissions. Only one Agreement is required per submission.

CORRESPONDING AUTHOR

Name:

Kristin S. Miller

Department:

Biomedical Engineering

Institution:

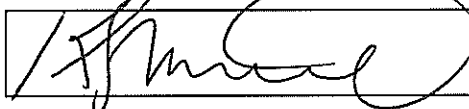
Tulane University

Title:

Assistant Professor

ARTICLE AND VIDEO LICENSE AGREEMENT

Signature:



Date:

4/12/2019

Please submit a **signed** and **dated** copy of this license by one of the following three methods:

1. Upload an electronic version on the JoVE submission site
2. Fax the document to +1.866.381.2236
3. Mail the document to JoVE / Attn: JoVE Editorial / 1 Alewife Center #200 / Cambridge, MA 02140

Editorial comments

General:

1. Please take this opportunity to thoroughly proofread the manuscript to ensure that there are no spelling or grammar issues.

Thank you for your feedback. We have revised and thoroughly proofread the manuscript.

2. JoVE cannot publish manuscripts containing commercial language. This includes trademark symbols (™), registered symbols (®), and company names before an instrument or reagent. Please limit the use of commercial language from your manuscript and use generic terms instead. All commercial products should be sufficiently referenced in the Table of Materials and Reagents.

For example: Excel, Nikon Eclipse, Myoview, Vevo2100

Thank you, the following changes have been made throughout the text to prevent any commercial product names.

“Excel” is now changed to “spreadsheet”

“Nikon Eclipse” was deleted

“Myoview,” is now referenced as “computer program”

“Vevo2100” is now termed “ultrasound system”

Protocol:

1. Please split up Protocol steps so that individual steps contain only 2–3 actions and a maximum of 4 sentences.

Thank you. The steps have either been revised or broken down into subsequent steps in order to comply with the 4-sentence maximum.

2. Being a video based journal, JoVE authors must be very specific when it comes to the humane treatment of animals. Regarding animal treatment in the protocol, please add the following information to the text:

a) Please include an ethics statement before all of the numbered protocol steps indicating that the protocol follows the animal care guidelines of your institution.

The requested ethics statement was added to section 1.1. of the protocol.

“1.1. Nulliparous 4-6 months female C57BL6J mice (29.4 ± 6.8 grams) at estrus were used for this study. All procedures were approved by the Institute Animal Care and Use Committee at Tulane University. After delivery, the mice were acclimated for one week before euthanasia and were housed under standard conditions (12-hour light/dark cycles).

b) Please specify the euthanasia method.

Thank you – we have clarified the euthanasia method. A hypoxic environment effects a variety of molecular mechanisms, which alter the smooth muscle tone in the female reproductive system^{1,2}. Further, anesthesia effects intracellular calcium concentrations,

inhibiting smooth muscle contractility³. Therefore, guillotine without anesthesia was selected for basal tone testing. This method of euthanasia is accepted to study smooth muscle function ⁴⁻⁷ Section 1.4. has been added to convey this message to the audience. If only passive testing is performed, then euthanizing using carbon dioxide inhalation is acceptable.

“1.4. Mice undergoing basal tone testing are euthanized via guillotine. Mice tested only under the passive conditions are euthanized using carbon dioxide (CO₂) inhalation. The guillotine serves to preserve the function of smooth muscle cells of the reproductive tract, as the CO₂ gas alters the contractile properties of the smooth muscle cells¹⁻⁷. It is imperative to perform the dissection within 30 minutes to minimize the chance of cell apoptosis.

c) Please do not highlight any steps describing euthanasia

The protocol was modified as requested. The highlighted portions now contain key steps to the dissection, the cannulation steps, and the mechanical testing process.

3. For each protocol step/substep, please ensure you answer the “how” question, i.e., how is the step performed? Alternatively, add references to published material specifying how to perform the protocol action. If revisions cause a step to have more than 2-3 actions and 4 sentences per step, please split into separate steps or substeps.

Thank you for the comment. We have modified the manuscript to address this.

Examples:

5.5. Finding the experimental in vivo stretch: Adjust the organ to be at the estimated in vivo length while at the unloaded pressure and press “start.” Assess pressure vs force values for pressure values ranging from the unloaded pressure to the maximum pressure (Table 1). Press the “stop” button in the computer program and save the file.

6.13. Calculate the unloaded thickness from ultrasound images B-mode image: Using an imaging software, draw a line to denote the penetration depth. Set the scale and then enter the length of the line (i.e. 2000 µm as shown in Figure 6B and 6D).

References:

1. Please ensure that the references appear as the following: [Lastname, F.I., LastName, F.I., LastName, F.I. Article Title. Source. Volume (Issue), FirstPage – LastPage (YEAR).] For more than 6 authors, list only the first author then et al.

The references have been modified and re-ordered. Example citations are included below.

- 1 [Capone, D., *et al.* Evaluating Residual Strain Throughout the Murine Female Reproductive System. *Journal of Biomechanics*. 82 299-306, (2019).]

- 2 [Danforth, D., The fibrous nature of the human cervix, and its relation to the isthmic segment in gravid and nongravid uteri. *American Journal of Obstetrics and Gynecology*. 53 (4), 541-560 (1947).]
- 3 [Hughesdon, P., The fibromuscular structure of the cervix and its changes during pregnancy and labour. *Journal of Obstetrics and Gynecology of the British Commonwealth*. 59 763-776 (1952).]
- 4 [Bryman, I., Norstrom, A. & Lindblo, B. Influence of neurohypophyseal hormones on human cervical smooth muscle cell contractility in vitro. *Obstetrics and Gynecology*. 75 (2), 240-243 (1990).]

Table of Materials:

1. Please ensure the Table of Materials has information on all materials and equipment used, especially those mentioned in the Protocol

Thank you—the table has been modified.

Name of Material/ Equipment	Company	Catalog Number	Comments/Description
Student Dumont #5 Forceps	Fine Science Tools	91150-20	straight forceps
Dumont SS Forceps	Fine Science Tools	11203-25	straight forceps
Dumont #5/45 Forceps	Fine Science Tools	11251-35	curved forceps
4-0 Suture	Fine Science Tools	18020-40	smaller suture ties
6-0 Suture	Fine Science Tools	18020-60	larger suture ties
Instrument Cases	Fine Science Tools	20830-00	casing to hold dissection tools
Student Vannas Spring Scissors	Fine Science Tools	91500-09	micro-scissors
Wagner Scissors	Fine Science Tools	14069-12	larger scissors
Force Transducer - 110P	Danish MyoTechnologies	100079	force transducer
Pressure Transducer	Danish MyoTechnologies	100106	pressure transducer
NaCl	VWR	97061-274	HBSS concentration: 8000 mg/mL KRB concentration: 70.1 g/L
KCl	Fisher Chemical	97061-566	HBSS concentration: 400 mg/ mL KRB concentration: 3.5 g/L
MgCl ₂ -6H ₂ O	VWR	BDH9244-500G	HBSS concentration: 100 mg/ mL
KH ₂ PO ₄	G-Biosciences	71003-454	HBSS concentration: 60 mg/ mL
Na ₂ HPO ₄ (dibasic anhydrous)	VWR	97061-588	HBSS concentration: 48 mg/mL KRB concentration: 1.44 g/L
MgSO ₄ -7H ₂ O	VWR	97062-134	HBSS concentration: 48 mg/ mL
CaCl ₂ (anhydrous)	VWR	97062-590	HBSS concentration: 140 mg/ mL
NaHCO ₃	VWR	97062-460	HBSS concentration: 350 mg/ mL KRB concentration: 21.0 g/L

Dextrose (D-glucose)	VWR	101172-434	HBSS concentration: 1000 mg/mL KRB concentration: 19.8 g/L
MgCl ₂	VWR	97064-150	KRB concentration: 1.14 g/L
CaCl ₂ ·2H ₂ O	Fischer chemical	BDH9224-1KG	KRB concentration: 3.68 g/L
Eclipse	Nikon	E200	microscope used for imaging
VEVO2100	FujiFilm Visual Sonics	VS-20035	ultrasound used for imaging
Ultrasound transducer	FujiFilm Visual Sonics	LZ-550	ultrasound transducer used; 256 elements, 40 MHz center frequency
Flow meter	Danish MyoTechnologies	161FM	flow meter within the testing apparatus
Pressure myograph systems	Danish MyoTechnologies	110P and 120CP	Pressure myograph system: program, cannulation device, and controller unit
Microsoft excel	Microsoft	6278402	program used for spreadsheet

Reviewer 1

Manuscript Summary:

This provides a nice description of a biaxial protocol for testing of the murine cervix and vagina. While the methods are somewhat specific to the use of technologies that will not be available in most labs, the details of the protocol are generalizable to protocols that utilize other technologies to accomplish similar measurements. Thus, the work is considered worthy of publication and a valuable contribution to the literature.

Major Concerns:

None

Minor Concerns:

1. Section 2. Could the authors comments on the time of dissection to maintain viability of the tissue and method of euthanasia?

Thank you for bringing this to our attention for this is a key component of the experiment. To maintain viability of the cells in the tissue, the organs must be dissected within 30 minutes postmortem. (With training, the reproductive system can be dissected within 15 minutes. A hypoxic environment effects a variety of molecular mechanisms, which alter the smooth muscle tone in the female reproductive system.^{1,2} Further, anesthesia effects intracellular calcium concentrations, which inhibits smooth muscle contractility.³ Therefore, guillotine without anesthesia was selected for basal tone testing. This method of euthanasia is accepted to study smooth muscle function.⁴⁻⁷ The text is revised to include the euthanasia method for each testing component and the factor of time when completing a basal tone test.

“1.4. Mice undergoing basal tone testing are euthanized via guillotine. Mice tested only under the passive conditions are euthanized using carbon dioxide (CO₂) inhalation. The guillotine preserves the function of smooth muscle cells of the reproductive tract, as the CO₂ gas alters the contractile properties of the

smooth muscle cells¹⁻⁷. It is imperative to perform the dissection within 30 minutes to minimize cell apoptosis.”

2. Section 2.8: perhaps say "post-explant length" here to keep consistent with the rest of the text. It would also be nice to refer to section 5 where this calculation is made.

Thank you for these suggestions. The text has been changed to post-explant length and section 5 is now referenced.

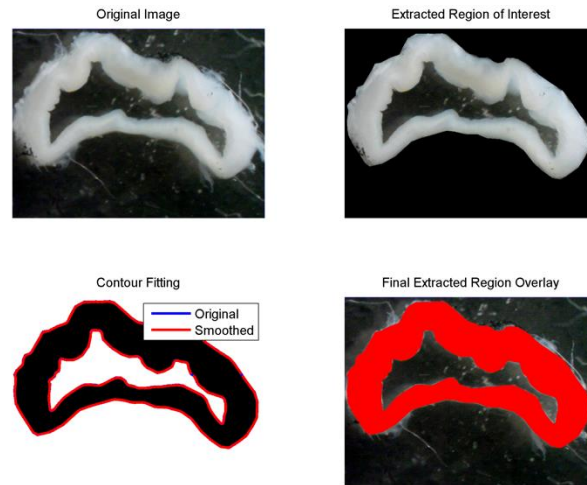
“2.9. Cut the uterine horns immediately inferior to the ovaries. Note that the organs will retract from the post explant length as the connective tissue is removed and the organ recoils. Place the dissected reproductive organs in a petri dish filled with 4°C HBSS. This change in length will be used in for calculating the estimated *in vivo* length (section 5).”

3. Line 223: word "stretch" is missing after "in vivo". The latter should also be in italics.

Thank you for catching this oversight. The correction is made to read “Adjust the organ to -2% *in vivo* length and press “start.” The term length was used in this passage to remain consistent with the text.

4. 6.13: Why not use an edge detection algorithm?

Thank you for thoughtful question. This was initially attempted, where the inner and outer diameter was traced and the edges between the 2 boundaries were detected. This worked well on vaginal cross section taken under a microscope, however, failed to work for the ultrasound images. Troubleshooting demonstrated the custom code was sensitive to the pixel value. For example, the tissue was generally a white color and if a black mark was made across the cross section the algorithm failed. Therefore, it was hypothesized since the ultrasound images are commonly pixelated with various pixel values the code had a difficult time extrapolating between the two points. Therefore, the same principle was applied and performed manually in ImageJ multiple times to minimize variability. This, however, can be further investigated to permit edge detection. Images added for reference.



5. Representative Results: It would be nice for the authors to provide the tangent moduli that were calculated.

Thank you for this suggestion. The requested data may now be found in Table 2.

	Vagina	Cervix
Basal Circumferential (kPa)	127.94	188
Basal Axial (kPa)	56.8	75.44
Passive Circumferential (kPa)	246.03	61.26
Passive Axial (kPa)	112.74	19.26

Table 2: The representative results for the physiologic pressure measured within the vagina and cervix. Pressure was taken during both basal and passive conditions as well as for both circumferential and axial directions. All measurements provided are in units of kPa.

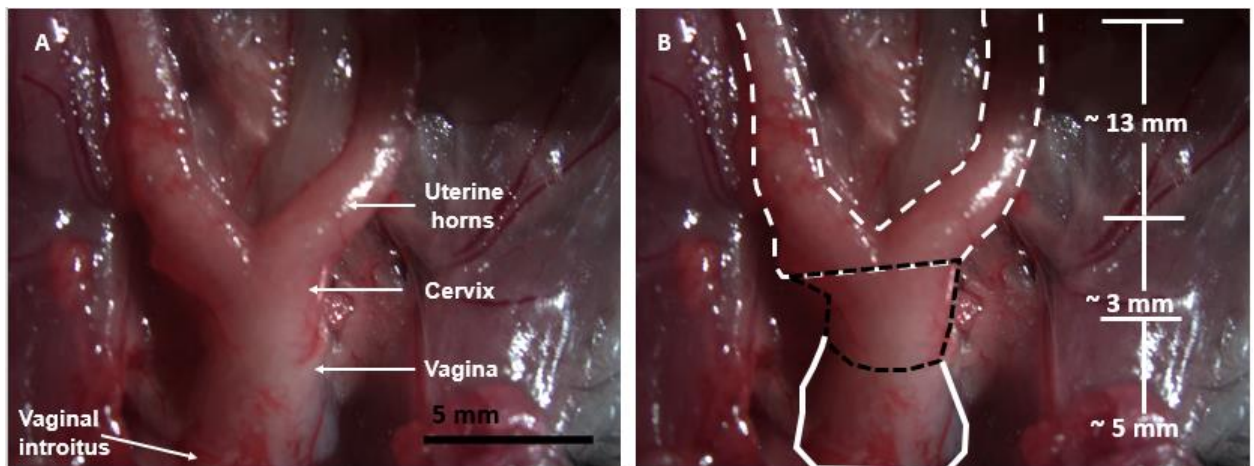
Reviewer 2

Major Concerns:

1. It is not clear how the authors distinguish between the cervix and vagina - It would be helpful if the authors included a description of how the cervix and vagina were excised from the rest of the reproductive tract in section 2.

Thank you for bringing this concern to us. The manuscript is now revised to have section 2.6. devoted to identifying the distinct differences between the cervix and vagina to appropriately separate them. Additionally, Figure 1 now serves as a diagram of the main reproductive organs with averaged in vivo lengths, which was measured by ImageJ technology.

“2.6. Identify the reproductive system: The uterine horns bifurcate from the cervix. The cervix can be identified from the vagina due to differences in geometry and stiffness. The outer diameter of the cervix is smaller than the vagina. The cervix is stiffer than the vagina and feels similar to that of a bead.”



The mouse dissection for the reproductive organs: both uterine horns, cervix, vagina and vaginal introitus (A). In the figure, the bladder and urethra are removed from the anterior of the vagina. The intestines and abdominal muscles have been reflected superiorly. The average in vivo lengths for the uterine horns, cervix, and vagina were calculated using ImageJ technology (B).

2. Section 5: I found this section to be confusing. In particular, there are multiple measurements of unloaded geometry and in vivo geometry mentioned throughout this section. An overview of the protocol would be nice at the beginning. For example, there are many places in which unloaded geometry is estimated/measured/re-evaluated. Unloaded geometry is very important, but as presented here, it's not clear what the "real" unloaded geometry is, or which measurements are used for the calculations in Section 8.

Thank you for your comments. We have revised section 5 per the reviewer's comments and the measurement of unloaded geometry has been clarified. Additionally, we have added lines in sections 5.9, 5.11, 5.14, and 5.18 that detail which measurements are used for calculations.

“5.9. Re-evaluate the unloaded geometry: Set the organ to the *in vivo* length and the pressure to the unloaded pressure. Decrease the axial length towards the estimated unloaded length at a rate of 10 $\mu\text{m/s}$ until there is minimal change in the force. This corresponding length is known as the unloaded length, where the

organ is not in tension nor compression. Before zeroing the force, record the unloaded length, outer diameter, and the force value.

NOTE: The prior unloaded geometry was determined by visual cues, which is purely qualitative. A re-evaluation is necessary for a quantitative method and to take into account the possible plastic deformations and changes in length that may occur during preconditioning. This geometry will be used in section 8.”

“5.11 Ultrasound Imaging: Identify the cannula near the force transducer and adjust the stage of the microscope to image along the length of the tissue. Throughout the testing process, the middle region along the length is tracked (**Figure 5A and 5C**). Following imaging, review the image “Cine store” loop that consists of a series of B-mode frames and identify the frame with the largest outer diameter. The thickness calculations made will be used in section 8.”

“5.14. Pressure diameter testing (+2% *in vivo* length): Adjust the organ so that is it +2% *in vivo* length, set the pressure to 0 mmHg, and gradient to 1.5 mmHg/s. Increase the pressure from 0 mmHg to the maximum pressure and then back down to 0 mmHg with a 20 second hold period. Repeat this for 5 cycles. The pressure data from all three lengths will be used in section 8.”

“5.18. Force-length testing (maximum pressure + UP): Set the pressure to the maximum pressure + UP and adjust the organ to -2% the *in vivo* length. At a rate of 10 $\mu\text{m/s}$ stretch the organ to +2% of the *in vivo* length and back to -2% the *in vivo* length. After repeating for a total of 3 cycles, save the data. All force data will be used in section 8.”

Within the manuscript, UP is defined as unloaded pressure.

Minor Concerns:

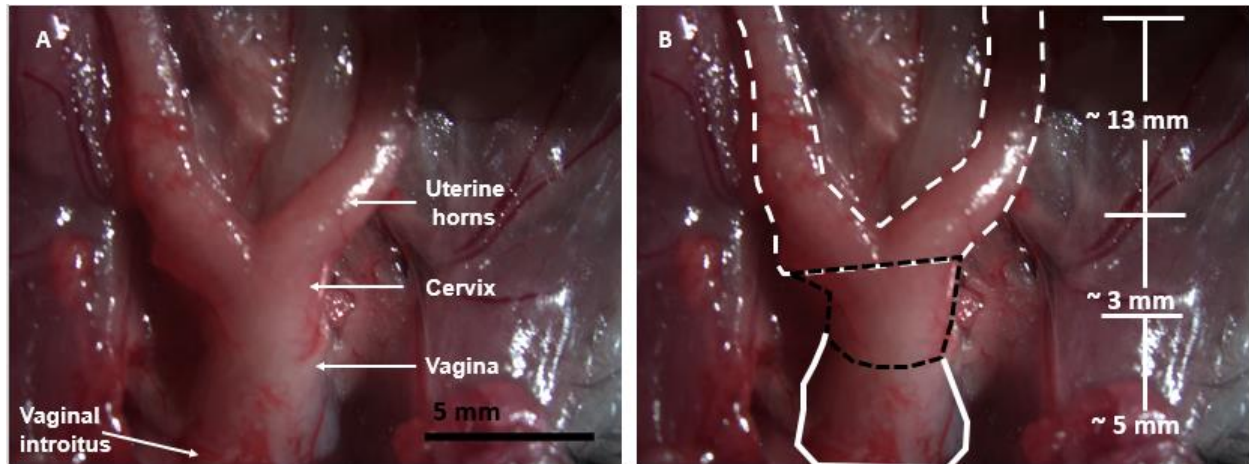
1. Please specify if the mice were nulliparous (virgin).

Thank you for bringing this detail to our attention. The animals used in this study were nulliparous. A section (1.1) has been added to included information on age, strain, weight, and parity.

“Nulliparous 4-6 months female C57BL6J mice (29.4 ± 6.8 grams) at estrus were used for this study. All procedures were approved by the Institute Animal Care and Use Committee at Tulane University. After delivery, the mice acclimated for one week before euthanasia and were housed under standard conditions (12-hour light/dark cycles).”

2. Please define vagina introitus in Figure 1

Thank you for the suggestion. Figure 1 now contains arrows and labels for the uterine horns, cervix, vagina, and vagina introitus.



The mouse dissection for the reproductive organs: both uterine horns, cervix, vagina and vaginal introitus (A). In the figure, the bladder and urethra are removed from the anterior of the vagina. The intestines and abdominal muscles have been reflected superiorly. The average in vivo lengths for the uterine horns, cervix, and vagina were calculated using ImageJ technology (B).

3. Section 3.2/3.3: A picture of how the sutures were tied down during the cannulation would be nice

Thank you for this suggestion. The figure has been added and is now Figure 3 within the text. Attached is the figure and corresponding figure caption.

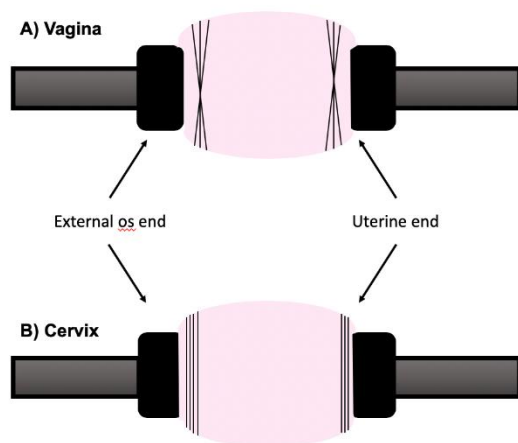


Figure 3: Cannulation Method for Vagina and Cervix

Due to the varying geometry and thickness of the reproductive organs, they are most effectively cannulated in distinct manners. For the vagina, place two sutures in an “X” fashion with a third directly in the intersection of the “X”. When cannulating the cervix, place 3 horizontal sutures on the uterine end and 4 sutures on the external os.

4. Basal tone testing - please introduce in more detail towards the beginning of the manuscript. This type of testing is not common in the reproductive biomechanics field. Details on what exactly basal tone mechanical testing measures would be helpful.

Thank you for this suggestion. An additional paragraph concerning the details of basal testing and how this differs from passive testing has been added to the introduction.

“The protocol is divided into two main mechanical testing sections: basal tone and passive testing. Basal tone is defined as the baseline partial constriction of smooth muscle cells, even in the absences of external local, hormonal, and neural stimulation⁸. This baseline contractile nature of the vagina and cervix yields characteristic mechanical behaviors which are then measured by the pressure myograph system. The passive properties are assessed by removing the intracellular calcium that maintains the baseline state of contraction resulting in relaxation of the smooth muscle cells. In the passive state collagen and elastin fibers provide the dominant contributions for the mechanical characteristics of the organs.”

Additionally, two paragraphs that describe the composition of the vaginal wall, in terms of the smooth muscle cell distribution and organization were added to the beginning.

“The vaginal wall is composed of four layers, the epithelium, lamina propria, muscularis, and adventitia. The epithelium is primarily composed of epithelial cells. The lamina propria has a large amount of elastic and fibrillar collagen fibers. The muscularis is also composed of elastin and collagen fibers but has an increased amount of smooth muscle cells. The adventitia is comprised of elastin, collagen, and fibroblasts, albeit in less concentrations as the previous layers. The smooth muscle cells are of interest to biomechanically motivated research groups as they play a role in the contractile nature of the organs⁹⁻¹¹. As such, quantifying the smooth muscle cell area fraction and organization is key to understanding the mechanical function. Previous investigations suggest that the smooth muscle content within the vaginal wall is primarily organized in the circumferential and longitudinal axis^{10,12,13}. Histological analysis suggests that the smooth muscle area fraction is approximately 35% for both the proximal and distal sections of the wall¹⁴.

The cervix is a highly collagenous structure, that until recently, was thought to have minimal smooth muscle cell content^{15,16}. Recent studies, however, suggest that smooth muscle cells may have a greater abundance, and role, in the cervix^{17,18}. The cervix exhibits a gradient of smooth muscle cells; the internal os contains 50-60% smooth muscle cells where the external os only contains 10%¹⁵. Mouse studies, however, report the cervix to be composed of 10-15% smooth muscle cells and 85-90% fibrous connective tissue with no mention of regional differences¹⁹⁻²¹. Given that the mouse model differs from the frequently reported human model, further investigations concerning the mouse cervix are needed.”

5. Section 5.4, line 202: How is in vivo pressure defined? Please reference Table 1

Thank you for the suggestion of referencing Table 1 in the script. The *in vivo* pressure used in this study is defined as the physiologic pressure that is normally experienced inside the lumen of the respective organs within the body. For both organs, catheterization was performed on C57BL6 mice under anesthesia (4% isoflurane in 100% oxygen) to obtain the unloaded pressure values reported within the manuscript. The use of a balloon catheter to measure the pressure inside of the vagina is reported on the rat and rabbit model^{22,23}. For measuring the cervical pressure, a 2F catheter was utilized. Further, a pilot study being conducted within our lab group is investigating the physiologic pressure of the cervix. We have estimated the cervical physiologic pressure to be 10 mmHg (± 2 mmHg). As this is a pilot study, further studies should investigate the physiologic pressure experienced by the cervix. This is addressed later in the document as being a limitation and as a direction for the field to take in the future.

Additionally, the description for Table 1 has been expanded to include this information.

“Table 1: Summary of Information for Scaling the Mechanical Testing Methods for Each Organ. The unloaded pressure values were measured using catheterization techniques under anesthesia (4% isoflurane in 100% oxygen). A balloon catheter was utilized for the vaginal measurements and a 2F catheter for the cervix.”

5. Section 5.5, line 206 please specify measured vs. estimated stretch.

Thank you for catching this generalization. To minimize the confusion the title of the paragraph was been adjusted to “Finding the experimental *in vivo* stretch”. The *in vivo* stretch was experimentally estimated by measuring the force values with the force transducer. Additionally, a note is now at the end of section 5.5 explaining that the difference between measured stretch and estimated stretch values. Estimated stretch is the theoretical recoil while the experimental stretch value is measured by the investigator.

5.5. Finding the experimental *in vivo* stretch: Adjust the organ to be at the estimated *in vivo* length while at the unloaded pressure and press “start.” Assess pressure vs force values for pressure values ranging from the unloaded pressure to the maximum pressure (Table 1). Press the “stop” button in the computer program and save the file.

NOTE: The measured stretch value is calculated *in situ*. This is accompanied by the limitation that it can only be measured after disarticulating the pubic symphysis. As a result, the natural tethering is lost, which may modify the length. The theoretical stretch, however, is based on the previously introduced theory that the organ will experience minimal changes in force when exposed to physiologic pressures to conserve energy²⁴. In the protocol, the measured *in vivo* stretch will be the stretch value calculated using the experimentally identified length wherein there is minimal change in force when exposed to a physiologic range of pressures.

6. Section 5.5, line 208: Please reference table for determining maximum pressure.

Thank you for the suggestion. The reference was added.

“5.5. Finding the experimental *in vivo* stretch: Adjust the organ to be at the estimated *in vivo* length while at the unloaded pressure and press “start.” Assess pressure vs force values for pressure values ranging from the unloaded pressure to the maximum pressure (Table 1). Press the “stop” button in the computer program and save the file.

7. How is the pressure-diameter pre-conditioning different between 5.4 and 5.6?

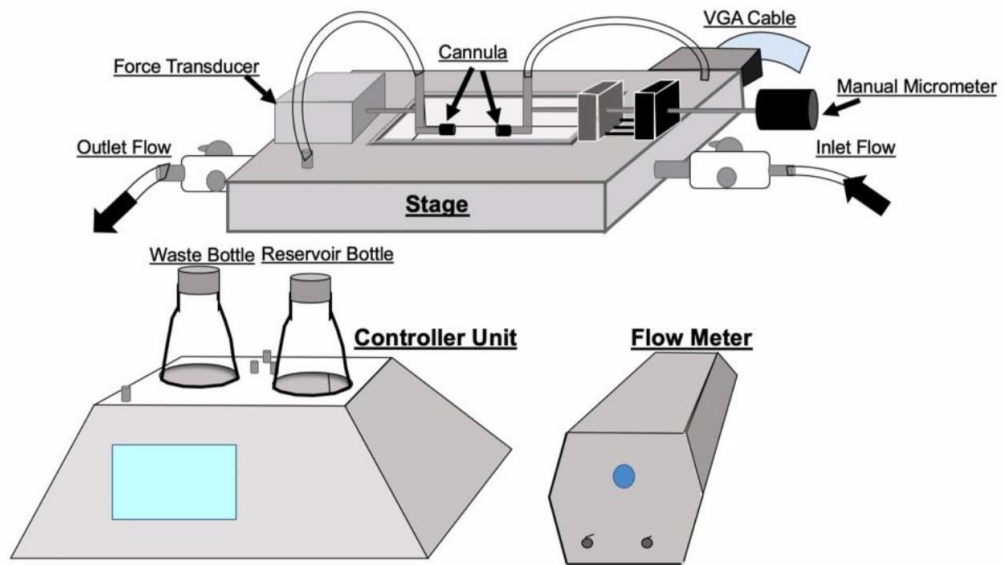
Thank you for the great question. In our experience, it is imperative to precondition the organs before identifying the corrected *in vivo* stretch in order to obtain consistent and repeatable force values. The first pressure-diameter pre-conditioning (5.4) is completed prior to finding the experimental *in vivo* stretch. Often, the *in vivo* stretch is initially underestimated since it is determined from measurements on organ recoil taken during dissection after disarticulating the pubic symphysis. The second round of pressure-diameter pre-conditioning (5.6) is performed after the experimental *in vivo* stretch is determined. Thus, we repeat the preconditioning protocol to ensure that hysteresis is minimized following the additional axial extension in order to ensure that results are consistent, repeatable, and mathematically interpretable.

The text was modified to include a note following section 5.6.

“NOTE: 5.4 is imperative in order to achieve a consistent and repeatable axial force reading with increasing pressure. This step aids in finding the correct *in vivo* stretch, which is often underestimated based on visual cues. 5.6 serves to minimize hysteresis and to achieve a consistent, repeatable, mathematically interpretable response of the organ following the potential increase in axial deformation.”

8. Line 222: what is P1 and P2?

Thank you for asking this question. P1 and P2 are within the program interface and sets the inlet (P1) and outlet pressure (P2) of the pressure myograph. The text has been modified to better reflect the inlet and outlet pressures of the protocol. The inlet and outlet pressure correspond to the inlet and outlet flow of the myograph system. The figure caption for Figure 4 is now revised to include this definition.



“The setup of the DMT device utilized for both basal and passive testing. The DMT is composed of three main hubs: the stage (A), controller unit (B), and flow meter (C). Within the controller unit, there is a reservoir bottle and a waste bottle. The reservoir bottle is initially filled with fluid that empties as the experiment is carried out. The waste bottle, which is initially empty, obtains the fluid that runs through the experiment. The controller unit interfaces with the DMT software on the computer and controls the pressure, temperature, and flow. The controller unit reads the outputs from the force and pressure transducers within the stage through a VGA interface cable. The stage component of the system contains an inlet and outlet flow of the system. The inlet and outlet flow have corresponding inlet and outlet pressures measured by the system.”

9. Section 6: How long was the tissue equilibrated after being frozen?

Thank you for your question. If an organ is being used for passive testing and was previously frozen, the organ is given a thirty-minute equilibration period at room temperature before being cannulated. A statement addressing this question is now added to the existing note in between section heading 6 and section 6.1.

“6. Passive Mechanical testing

NOTE: If starting with passive testing start at step 1. If basal tone testing was performed prior to passive start at step 6. If the organ was frozen, allow a 30-minute equilibration period at room temperature before cannulating the organ.”

10. Section 7: Is the opening angle measurements used in the analysis in section 8? What are some of the representative results from this test?

Opening angle measurements are not used in the measurements calculated in the previous section 8. Opening angle measures the residual strain, or the strain the organ experiences when all external loads are removed²⁶, and is a helpful tool for accurate 3D mathematical models¹⁴. Further, opening angle experiments may be used to measure the unloaded thickness in the event ultrasound is not available²⁷. After careful consideration, the text portions concerning opening angle measurements were removed to improve clarity.

11. 6.4: What is the suggested rate for preconditioning?

The rate is 1.5 mmHg/s for the passive testing pressure-diameter testing. 1.5 mmHg/s was previously used in literature to minimize rapid pressurization to the smooth muscle cells²⁸. The text was revised to include this.

“6.4. Pressure diameter pre-conditioning: After pressing “start”, set the pressure set to 0 mmHg, the length as the estimated *in vivo* length, and gradient to 1.5 mmHg/s²⁸. Begin running a sequence that takes the pressure from 0 mmHg to the maximum pressure and back to 0 mmHg. This process should be repeated through 5 cycles with a 30 second hold time.”

12. In section 8, please specify where the unloaded geometry measurements are coming from. What is the difference between the unloaded radius, R0 and r0? At which steps were R0 and r0 determined?

Thank you for the comment.

The unloaded dimensions consist of the unloaded thickness, radius, and length. The unloaded thickness is calculated from the ultrasound images while at the unloaded length and unloaded pressure (Fig 5). The unloaded length is measured with digital calipers from suture to suture. The unloaded diameter is measured via the microscope, camera, and software (Fig 5) followed by calculation of the radius. The manuscript is updated with these details.

“8.6. Find the unloaded volume of the organ (V). Equation 1 can be utilized to find V , given that R_0^2 is the unloaded outer radius measured by the microscope, L is the unloaded length, and H is the unloaded thickness as quantified by the ultrasound. The assumption of incompressibility is leveraged, meaning that it is assumed that the organ conserves volume while subjected to deformations.

NOTE: “The unloaded length is measured with calipers from suture to suture. The unloaded diameter is measured via the microscope, camera, and software followed by calculation of the radius (Figure 4). The unloaded thickness is calculated from the ultrasound images (Figure 5).”

- a) R_0 is the outer diameter in the original, unloaded configuration unloaded radius, which is defined as no external loads being applied to the organ/tissue. r_0 is the

deformed outer radius once exposed to externally applied loads, such as pressure or axial extension.

- b) R0 is determined in step 5.9 (basal testing) and 6.9 (passive testing). r0 is determined during real-time pressure-diameter and force-length testing. Within the computer program interface, there is a component dedicated to tracking the outer diameter of the organ being tested. The outer radius may then be extracted from the tracked outer diameter.

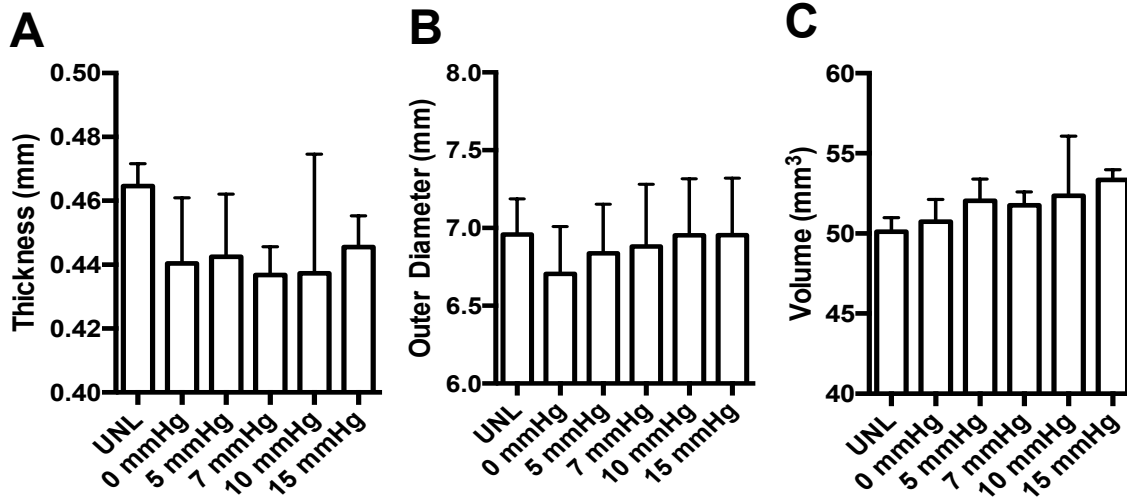
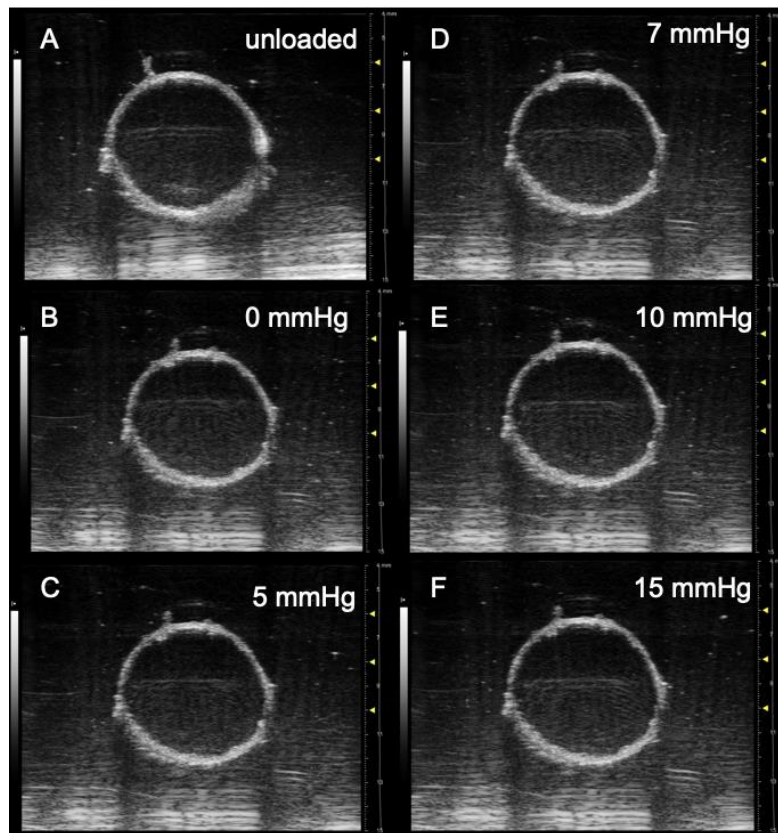
11. Line 622: Reference 45 did not test murine cervical tissue.

Thank you for catching that mistake. The sentence using the citation was framing the use of catheter studies within the reproductive system. The reference tested uterine tissue but as this paper is concerned with the vagina and cervix, this may be confusing. The paper and related references were adjusted to reflect only studies in the uterus, vagina, and cervix. Models include the mouse, rabbits and humans^{22,29-32}.

“Pressure catheterization is a method used previously to monitor the in vivo conditions within the vagina, cervix, and uterus^{22,29-32}. Models in the previous studies range from mice, rabbits, and humans. Herein, we leverage the methods introduced in these studies to quantify pressure in the mouse cervix and vagina^{29,32}.”

12. Discussion: Did the authors measure real-time changes in thickness? If so, can they calculate how the tissue volume changes and suggest whether or not the incompressibility assumption is valid?

Thank you for this insightful comment. Within this study the authors did not measure real-time changes in thickness. Thickness was solely measured at the unloaded configuration, as motivated by prior studies that demonstrate nonpregnant murine tissue exhibits minimal changes in volume during osmotic loading³³. Additionally, several additional studies have operated under the same assumption³⁴⁻³⁶. The authors, however, are performing a pilot study with the ultrasound system to measure real-time changes in thickness with pressurization to determine if the incompressibility assumption is valid. Initial results may be found below (n=2) which did not identify statistically significant differences in volume over a range of pressures. We are happy to include this pilot study in the manuscript at the editor's and reviewer's discretion.



Ultrasound imaging was performed with a 40MHz transducer on vaginal tissue (n=2) at the unloaded configuration (A) and the in vivo stretch (physiological length) at 0 B), 5 (C), 7 (D), 10 (E), and 15 (F) mmHg with basal tone. The calculated volume is reported as a function of loading (G). A one-way ANOVA with Tukey post hoc revealed no significant differences in volume with loading. Data reported as mean \pm standard error of mean. Additional analysis, including an increase in sample size, is needed to validate if the tissue is nearly incompressible.

The discussion portion is modified to address this limitation and possible future directions.

“A second limitation is assuming the organs are incompressible. Within this study, thickness was solely measured at the unloaded configuration, as motivated by prior studies that demonstrate nonpregnant murine tissue exhibits minimal changes in volume during osmotic loading⁶⁰. Furthermore, additional studies have operated under the same assumption of incompressibility^{31,41,61}. Ideally, ultrasound would be performed for the entirety of the experiment in order to remove the incompressibility assumption and to better inform finite element models”.

Reviewer 3

1. Section 1.1. I don't have any experience in determining estrous cycle and have a few clarification questions. Are the female murine genitals readily visible or does visualization require positioning the mouse in a specific orientation? The descriptions of the genitals in different stages is qualitative...is it difficult to determine stage of the cycle or are the described changes quite obvious?

Thank you for your questions. The external murine genitals are visible after lifting up the animal's tail. The stage of the estrous cycle is not difficult to determine, as the swelling and redness is quite distinct with each stage. Though, guides are available if an investigator was interested in training. Such references show examples of how mice strains appear at each estrous timepoint^{23,37,38}

Additionally, some references aim to compare alternatives such as vaginal cytology³⁷. Vaginal cytology is a way to observe the morphology of cells at different time points³⁹. As the epithelium is responsive to sex steroids, the cells undergo predictable changes for each timepoint in the estrous cycle. For example, the rising estrogen levels cause the vaginal epithelium to become large and flat while having small to absent nuclei^{37,40,41}.

There is a guide that was made by the Jackson lab that serve as an aid for determining the stage of estrous that make the stages quite distinct from the others. The guide has been inserted below and referenced in the text for visual cues. Vaginal cytology is regarded as the most accurate method for identifying the stage of estrous⁴².

The text is revised to include additional references and resources for training staff to determine and monitor estrous cycle.

“1.2. Determine the estrous cycle: The estrous cycle was monitored by visual assessment in accordance to previous studies^{37,41} and can be divided into four stages: proestrus, estrus, metestrus, and diestrus. During the proestrus phase the genitals are swollen, pink, moist, and wrinkled. Similarly, the estrus phase is wrinkly but less swollen, pink, and moist. Metestrus and diestrus are both reported as exhibiting no swelling and wrinkling, lacking in a pink hue, and dry^{42,43}.”

1.3. Perform experiment at estrus: All mechanical tests were performed while the mice were at estrus, as this is the easiest to visualize and provides a consistent and repeatable timepoint.”

2. Section 1.1. You should probably mention that the animal is sacrificed (at estrus) before proceeding with the subsequent work. Otherwise, the beginning of 2.1 is not clear if you are describing a live or dead animal.

Thank you for your feedback. That is a very good point and the change is made to section 1.1.

“1.1. Nulliparous 4-6 months female C57BL6J mice (29.4 ± 6.8 grams) at estrus were used for this study. All procedures were approved by the Institute Animal Care and Use Committee at Tulane University. After delivery, the mice acclimated for one week before euthanasia and were housed under standard conditions (12-hour light/dark cycles).”

3. Sections 2.6-2.7. Is it necessary to keep the tissues moist with HBSS during these dissection steps? It seems as though these tissues would dry out rather quickly if not monitored and hydrated.

We agree that this was a concern when handling soft biological tissues. If the tissue is dissected within 30 minutes, we have observed that the organs maintain their moisture content. A longer dissection time, however, may result in the tissue drying out. We have added in a note of having optional HBSS in a syringe that could then be used to add moisture to the tissue during dissection – which may be necessary for researchers in the initial stages of dissection training.

“NOTE: In order to ensure that the organs remain moist during the dissection, a syringe filled with 4°C HBSS may be used to add moisture to the organs.”

4. Section 2.8. Is the HBSS at room temperature or does it need to be maintained at body temperature?

Thank you for your question. At this stage of the experiment the HBSS is at 4°C. At this temperature, the solution pH is at 7.4 which is important for maintaining the viability of the smooth muscle cells. Once the organ has been cannulated, and the myograph system powered on, the media is replaced with body temperature KRB solution. The change in media is to preserve the pH of the organ. As the stage is not connected to the

system during the cannulation process, the colder HBSS is needed. Section 2.9 is revised to include a statement on this.

“2.9. Cut the uterine horns immediately inferior to the ovaries. Note that the organs will retract from the post explant length as the connective tissue is removed and the organ recoils. Place the dissected reproductive organs in a petri dish filled with 4°C HBSS. This change in length can be used in for calculating the estimated in vivo length (section 5).

NOTE: We have identified that using HBSS at this temperature during the dissection and cannulation does not affect the smooth muscle cell viability. Maintaining a pH of 7.4, however, is imperative for maintaining the viability of the smooth muscle cells. At this temperature the HBSS has a pH level of 7.4. “

5. Section 2.9. The sentence starting with "Noting that..." is not a complete sentence.

Thank you, the sentence has been corrected.

“Note that the organs will retract from the post explant length as the connective tissue is removed and the organ recoils.”

6. Section 3.1. The instructions are to "Determine the proper cannula size" but then the two sizes are specified. Will these sizes work for any strain/age of mouse or does each investigator actually need to "determine" the appropriate size as indicated? This is not clear.

Thank you for your questions about the cannula size as this is a key step for having a successful experiment. The specified sizes are the sizes used for a typical nulliparous 4-6 months C57-BL/6 murine vagina and cervix. The authors have used the same cannula size for nulliparous 4-6 months C57BL/6 x 129SvEv murine vagina. However, certain circumstances, such as prolapse or pregnancy, may require a larger size cannula. In this event the investigator would need to determine the size. Based on previous observations for the laboratory group, the same cannula size may be used for nonparous mice aged 4-13 months. The manuscript has been adjusted to reflect possible considerations for determining cannula size.

“3.1. Determine the proper cannula size for the organ type. In a typical C57BL6J mouse, the vagina uses cannulas that are both 3.75 mm in diameter and riveted. The cervix uses one cannula that is 3.75 mm for the vaginal end and a cannula 0.75 mm in diameter for the uterine end **(Figure 2)** The 0.75mm cannula is smooth.

“NOTE: The diameter sizes denoted above are used for typical nulliparous 4-6 months C57-BL/6 mice, C57BL/6 x 129SvEv, and nonparous mice aged 4-6 months. However, certain circumstances, such as prolapse or pregnancy, may require a larger size cannula.”

7. Section 3.3. The suturing process is not entirely clear. I suggest including a figure that visually demonstrates the suturing technique.

Thank you for this suggestion. The figure has been created and is now Figure 3 within the text. Attached is the figure and corresponding figure caption.

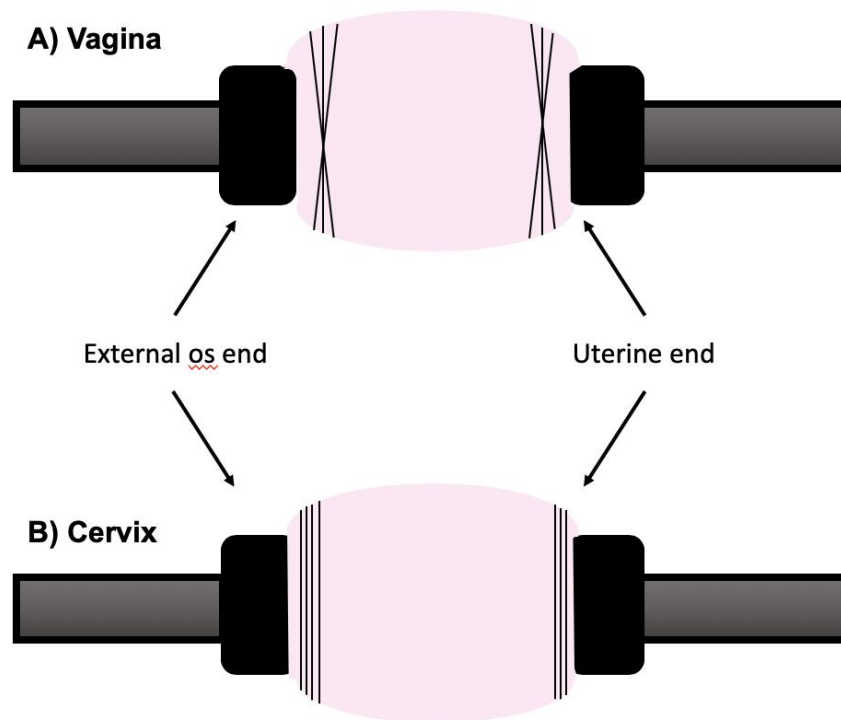


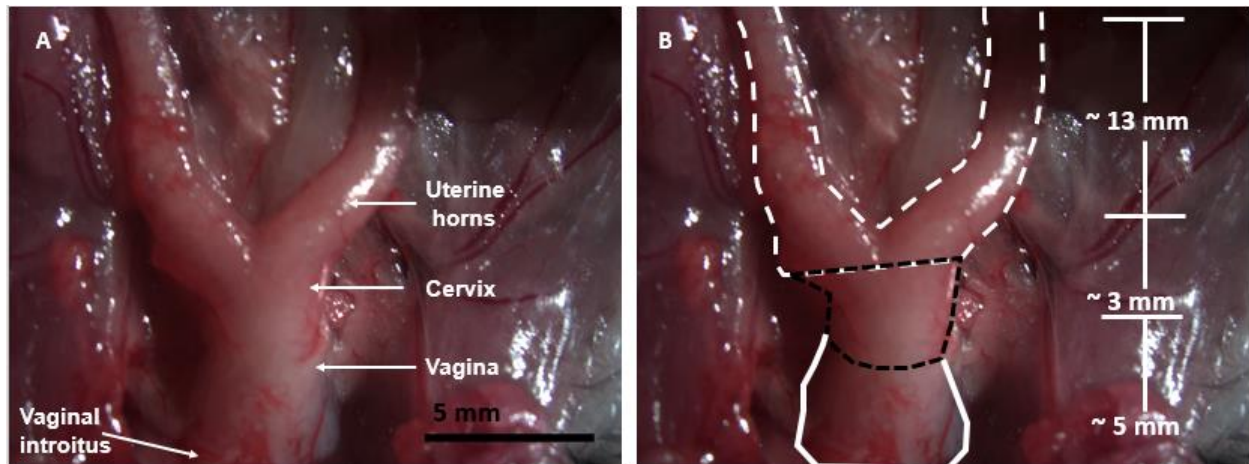
Figure 3: Cannulation Method for Vagina and Cervix

Due to the varying geometry and thickness of the reproductive organs, they are most effectively cannulated in distinct manners. For the vagina, place two sutures in an “X” fashion with a third directly in the intersection of the “X”. When cannulating the cervix, place 3 horizontal sutures on the uterine end and 4 sutures on the external os.

8. Section 5.1. There are several grammatical errors in this section, which made it a bit difficult to understand fully. It's not clear what is meant by the "singular cuts"? What is this and how are these performed?

Thank you for the grammar comment. To clarify, “singular cut” in this context denotes one incision made in order to excise the cervix. Further, we have carefully revised this section to make it clearer and more concise. Additionally, Figure 1 is revised to show the clear sections between the vagina and cervix. Lines are drawn onto Figure 1B to show where incisions would be made to excise the vagina or cervix.

“For the cervix, cut immediately below the ink dots that located above and below the central cervix mark. This ensures a cervical *in situ* length of 6 mm³⁵.”



The mouse dissection for the reproductive organs: both uterine horns, cervix, vagina and vaginal introitus (A). In the figure, the bladder and urethra are removed from the anterior of the vagina. The intestines and abdominal muscles have been reflected superiorly. The average *in vivo* lengths for the uterine horns, cervix, and vagina were calculated using ImageJ technology (B).

The section in its entirety now reads, “5.1. Finding the unloaded geometry: Stretch the organ so that the wall is not in tension. For the vagina, observe the grooves on the vaginal wall. For the cervix, cut immediately below the ink dots that located above and below the central cervix mark. This devises a repeatable method for a cervical *in situ* length of 6 mm³⁵. Measure the length from suture to suture with calipers.”

9. Section 5.7. Some of the text here could be cleaned up a bit (e.g., “below the *in vivo*” length?).

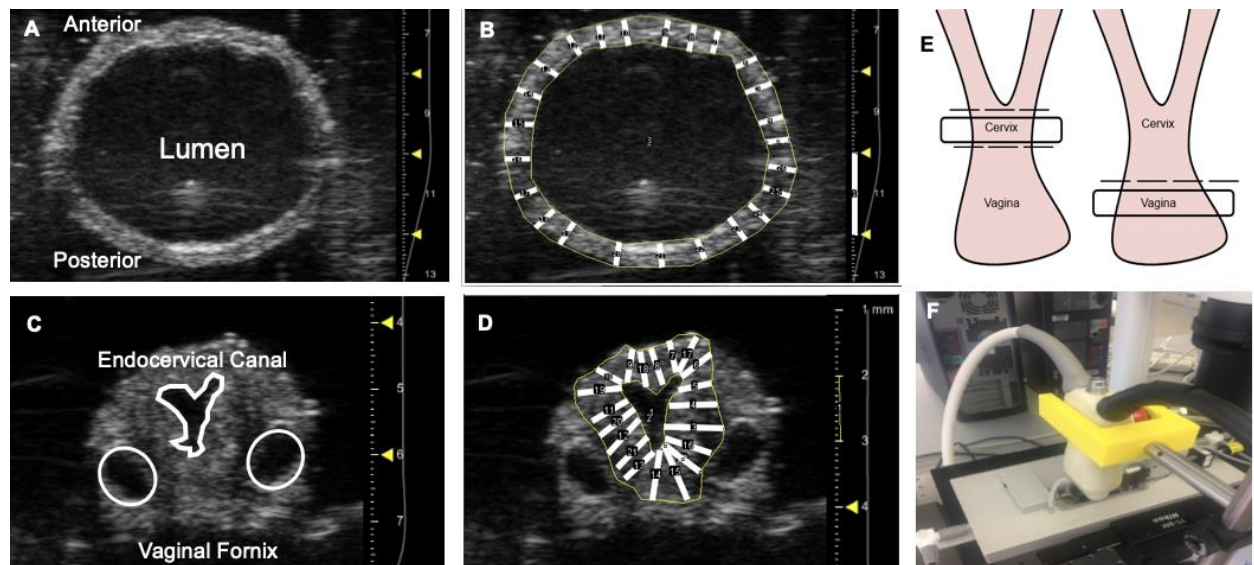
We appreciate the specific examples and have adjusted for the manuscript. This section has been reworded with primary changes of changing “2% below the *in vivo*” to “-2 of the *in vivo*”

“5.7. Force-length pre-conditioning: Enter 1/3 max pressure + UP for both the inlet and outlet pressure. Adjust the organ to -2% *in vivo* length and press “start.” Adjust the length to +2% *in vivo* length then back down to -2% at 10 μ m/s. Repeat axial extension for a total of 5 cycles. Press “stop” in the computer program and save the file.”

UP is defined within the manuscript as unloaded pressure.

10. Section 5.10. It might be helpful to show an image of the custom 3D printed holder.

Thank you for this suggestion. Figure 6 now contains a panel (E) which shows the 3D printed holder. Attached is the updated Figure for reference.



11. Section 5.14. Wording needs some editing (e.g., "Set the pressure to the pressure"?).

Thank you for bringing this to our attention, the section has been reworded to reflect that the pressure is the unloaded pressure. Other phrases were adjusted.

"5.14. Pressure diameter testing (+2% *in vivo* length): Adjust the organ so that it is +2% *in vivo* length, set the pressure to 0 mmHg, and gradient to 1.5 mmHg/s. Increase the pressure from 0 mmHg to the maximum pressure and then back down to 0 mmHg with a 20 second hold period. Repeat this for 5 cycles. The pressure data from all three lengths will be used in section 8."

12. General question. Why are some tests repeated for three cycles while others are repeated for five cycles?

Thank you for this question. The number of cycles were selected based on the minimum cycles needed to minimize hysteresis and Mullins effect for each test (pressure-diameter and fore length). For pressure-diameter testing (-2%, *in vivo*, +2%) a total of 5 cycles were needed to achieve a consistent and repeatable response. However, for the force-length testing (nominal, 1/3, 2/3, maximum pressure) a total of 3 cycles were needed to achieve a consistent and repeatable response.

13. Section 6.9. "Unloaded" is misspelled.

Thank you for identifying this grammatical error. The error is corrected in the text.

14. Section 8.1. Should be "data were collected".

Thank you for identifying this grammatical error. The error is corrected in the text.

15. Section 8.6. The tissue can be assumed to be incompressible or the volume can be assumed to be constant, but the volume can't be assumed to be incompressible.

Thank you for catching this. The manuscript has been adjusted to read that the organ is assumed to be incompressible rather than the volume.

16. Section 9. I suggest moving the "Clean Up" section before the "Data Analysis" section.

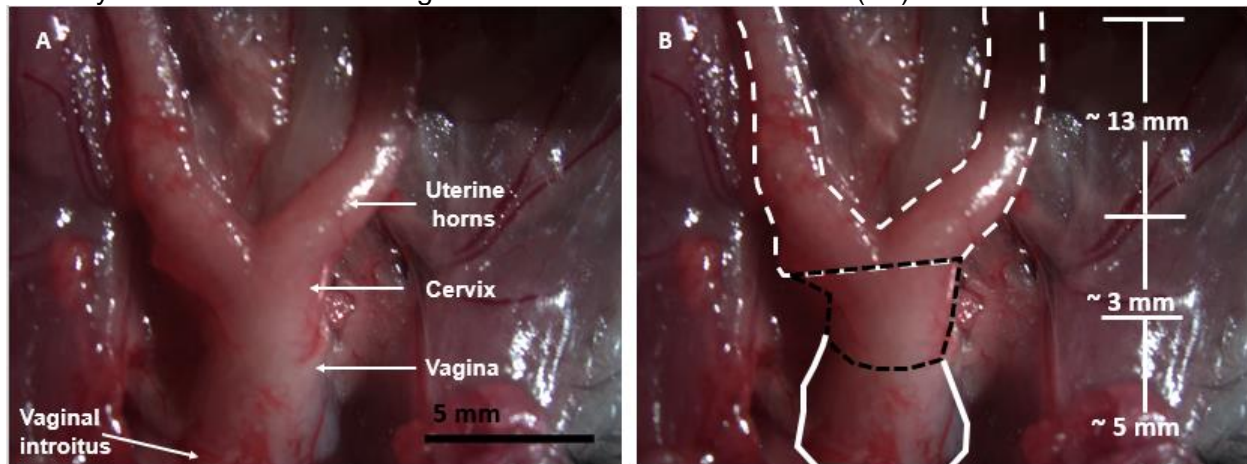
Thank you for this suggestion. The "Clean Up" section is now before the "Data Analysis" section.

17. Discussion. Many sentences have grammatical errors or missing words (e.g., lines 595-596, line 600, line 604, line 607, line 626, line 628, line 629). I suggest careful proofreading of the entire manuscript.

Thank you for the comment and the time you took to provide the specific examples. The manuscript was edited.

18. Figure 1. Should include scale bar for this image.

Thank you for the comment—Figure 1 now contains a scale bare (1A).



- 1 Bugg, G., Riley, M., Johnston, T., Baker, P. & Taggart, M. Hypoxic inhibition of human myometrial contractions in vitro: implications for the regulation of parturition. *Eur J Clin Invest.* **36** (2), 133-140 (2006).
- 2 Taggart, M. & Wray, S. Hypoxia and smooth muscle function: key regulatory events during metabolic stress. *Journal of Physiology.* **509** 315-325, doi:10.1111/j/1469-7793.1998.315bn.x, (1998).
- 3 Yoo, K. *et al.* The effects of volatile anesthetics on spontaneous contractility of isolated human pregnant uterine muscle: a comparison among sevoflurane, desflurane, isoflurane, and halothane. *Anesthesia and Analgesia.* **103** (2), 443-447, doi:10.1213/01.ane.0000236785.17606.58, (2006).

- 4 de Souza, L. *et al.* Effects of redox disturbances on intentional contractile reactivity in rats fed with a hypercaloric diet. *Oxidative Medicine and Cellular Longevity*. **2018**, doi:10.1155/2018/6364821, (2018).
- 5 Jaue, D., Ma, Z. & Lee, S. Cardiac muscarinic receptor function in rats with cirrhotic cardiomyopathy. *Hepatology*. **25** 1361-1365, doi:10.1002/hep.510250610, (1997).
- 6 Xu, Q. & Shaffer, E. The potential site of impaired gallbladder contractility in an animal mode of cholesterol gallstone disease. *Gastroenterology*. **110** (1), 251-257 (1996).
- 7 Rodriguez, U. *et al.* Effects of blast induced Neurotrauma on pressurized rodent middle cerebral arteries. *Journal of Visualized Experimentals*. **146**, doi:10.3791/58792, (2019).
- 8 Mohram, D. & Heller, L. in *Cardiovascular Physiology* Ch. 7, (The McGraw-Hill Companies, 2006).
- 9 Northington, G., Basha, M., Arya, L., Wein, A. & Chacko, S. Contractile Response of Human Anterior Vaginal Muscularis in Women With and Without Pelvic Organ Prolapse. *Journal of Reproductive Science*. **18** (3), 296-303, doi:10.1177/1933719110392054, (2011).
- 10 Basha, M. *et al.* Functional significance of muscarinic receptor expression within the proximal and distal rat vagina. *American Journal of Physiology. Regulatory, Integrative, Comparative Physiology*. **297** (5), (2009).
- 11 Boreham, M., Wai, C., Miller, R., Schaffer, J. & Word, R. Morphometric analysis of smooth muscle in the anterior vaginal wall of women with pelvic organ prolapse. *American Journal of Obstetrics and Gynecology*. **187** (1), 56-63 (2002).
- 12 Skoczylas, L. *et al.* Regional differences in rat vaginal smooth muscle contractility and morphology. *Reproductive Sciences*. **20** (4), 382-390 (2013).
- 13 Basha, M. *et al.* Regional differences in myosin heavy chain isoform expression and maximal shortening velocity of the rat vaginal wall smooth muscle. *American Journal of Physiology. Regulatory, Integrative, and Comparative Physiology*. **291** (4), (2006).
- 14 Capone, D. *et al.* Evaluating Residual Strain Throughout the Murine Female Reproductive System. *Journal of Biomechanics*. **82** 299-306, doi:10.1016/j.jbiomech.2018.11.001, (2019).
- 15 Danforth, D. The fibrous nature of the human cervix, and its relation to the isthmic segment in gravid and nongravid uteri. *American Journal of Obstetrics and Gynecology*. **53** (4), 541-560 (1947).
- 16 Hughesdon, P. The fibromuscular structure of the cervix and its changes during pregnancy and labour. *Journal of Obstetrics and Gynecology of the British Commonwealth*. **59** 763-776 (1952).
- 17 Bryman, I., Norstrom, A. & Lindblo, B. Influence of neurohypophyseal hormones on human cervical smooth muscle cell contractility in vitro. *Obstetrics and Gynecology*. **75** (2), 240-243 (1990).
- 18 Joy, V. *et al.* A New Paradigm for the Role of Smooth Muscle Cells in the Human Cervix. *Obstetrics*. **215** (4), 478.e471-478.e411, doi:10.1016/j.ajog.2016.04.053, (2016).
- 19 Xu, X., Akgul, Y., Mahendroo, M. & Jerschow, A. Ex vivo assessment of mouse cervical remodeling through pregnancy via Na (23) MRS. *NMR Biomedical*. **23** (8), 907-912 (2014).

- 20 Leppert, P. Anatomy and Physiology of cervical ripening. *Clinical Obstetrics and Gynecology*. **2000** (43), 433-439 (1995).
- 21 Schlembach, D. *et al.* Cervical ripening and insufficiency: from biochemical and molecular studies to in vivo clinical examination. *2009*. **144** S70-S79 (2000).
- 22 Park, K. *et al.* Vasculogenic female sexual dysfunction: the hemodynamic basis for vaginal engorgement insufficiency and clitoral erectile insufficiency. *International Journal of Impotence Journal*. **9** (1), 27-37 (1997).
- 23 Cason, A., Samuelsen, C. & Berkley, K. Estrous changes in vaginal nociception in a rat model of endometriosis. *Hormones and Behavior*. **44** (2), 123-131 (2003).
- 24 Van loon, P. Length-Force and Volume-Pressure Relationships of Arteries. *Biorheology*. **14** (4), 181-201 (1977).
- 25 Pena, E. *et al.* Mechanical characterization of the softening behavior of human vaginal tissue. *Journal of Mechanical Behavior of Biomedical Materials*. **4** (3), 275-283, doi:10.1016/j.mbbm.2010.10.006, (2011).
- 26 Chuong, C. & Fung, Y. On residual stresses in arteries. *Journal of Biomechanical Engineering*. **108** (2), 189-192 (1986).
- 27 Alford, P., Humphrey, J. & Taber, L. Growth and Remodeling in a thick-walled artery model: effects of spatial variations in wall constituents. *Biomechanical Modeling Mechanobiology*. **7** (4), 245-262 (2008).
- 28 Zhou, B., Rachev, A. & Shazly, T. The biaxial active mechanical properties of the porcine primary renal artery. *Journal of Mechanical Behavior and Biomedical Materials*. **48** 28-37 (2015).
- 29 Rada, C., Pierce, S., Grotegut, C. & England, S. Intrauterine Telemetry to Measure Mouse Contractile Pressure *In Vivo Journal of Visual Experiments*. (98), doi:10.3791/52541, (2015).
- 30 Lumsden, M. A. & Baird, D. T. Intra-uterine pressure in dysmenorrhea. *Acta Obstetricia et Gynecologica Scandinavica*. doi:10.3109/00016348509154715 (1985).
- 31 Milsom, I., Andersch, B. & Sundell, G. The Effect of Flurbiprofen and Naproxen Sodium On Intra-Uterine Pressure and Menstrual Pain in Patients With Primary Dysmennorrhea. *Acta Obstetricia et Gynecologica Scandinavica*. doi:10.3109/00016349809004294, (1988).
- 32 Bulletti, C. *et al.* Uterine Contractility During Menstrual Cycle. *Human Reproduction*. **15** 81-89 (2000).
- 33 Myers, K., Socrate, S., Paskaleva, A. & House, M. A Study of the Anisotropy and Tension/Compression Behavior of Human Cervical Tissue. *American Society of Mechanical Engineers*. **132** (2), doi:10.1115/1.3197847, (2009).
- 34 Murtada, S., Ferruzzi, J., Yanagisawa, H. & Humphrey, J. Reduced Biaxial Contractility in the Descending Thoracic Aorta of Fibulin-5 Deficient Mice. *Journal of Biomechanical Engineering*. **138** (5), doi:10.1115/1.4032938, (2016).
- 35 Robison, K., Conway, C., Desrosiers, L., Knoepp, L. & Miller, K. Biaxial Mechanical Assessment of the Murine Vaginal Wall Using Extension-Inflation Testing. *Journal of Biomechanical Engineering*. **139** (10), doi:10.1115/1.4037559, (2017).

- 36 Akintunde, A. *et al.* Effects of Elastase Digestion on the Murine Vaginal Wall Biaxial Mechanical Response. *American Society of Mechanical Engineers*. **141** (2), doi:10.1115/1.4042014, (2018).
- 37 Byers, S., Wiles, M., Dunn, S. & Taft, R. Mouse Estrous Cycle Identification Tool and Images. *Public Library of Science*. **7** (4), doi:<https://doi.org/10.1371/journal.pone.0035538>, (2012).
- 38 Champlin, A. Determining the Stage of the Estrous Cycle in the Mouse by the Appearance. *Biology of Reproduction*. **8** (4), 491-494, doi:doi:10.1093/biolreprod/8.4.491., (1973).
- 39 Cora, M., Kooistra, L. & Travlos, G. Vaginal cytology of the laboratory rat and mouse: review and criteria for the staging of the etrous cycle using stained vaginal smears. *Sage Journals*. **43** (6), 776-793 (2015).
- 40 Goldman, J., Murr, A. & Cooper, R. The rodent estrous cycle: characterization of vaginal cytology and its utility in toxicological studies. *Birth Defects*. **80** 84-97 (2007).
- 41 McLean, A. Performing Vaginal Lavage, Crystal Violet Staining and Vaginal Cytological Evaluation for Mouse Estrous Cycle Staging Identification. *Journal of Visualized Experiments*. **67**, doi:10.3791/4389., (2012).
- 42 Byers, S. Mouse Estrous Cycle Identification Tool and Images. *PLoS ONE*. **7** (4), doi:doi:10.1371/journal.pone.0035538, (2012).
- 43 Nelson, J., Felicio, P., Randall, K., Sims, C. & Finch, E. A Longitudinal Study of Estrous Cyclicity in Aging C57/6J Mice: Cycle, Frequency, Length, and Vaginal Cytology. *Biology Reproduction*. (1982).